ECSS-E-20-01A
5 May 2003

Space engineering

Multipaction design and test

ECSS Secretariat
ESA-ESTEC
Requirements & Standards Division
Noordwijk, The Netherlands

Published by: ESA Publications Division
ESTEC, P.O. Box 299,
2200 AG Noordwijk,
The Netherlands

ISSN: 1028-396X

Price: € 20

Printed in The Netherlands

Foreword

This standard is one of the series of ECSS standards intended to be applied together for the management, engineering and product assurance in space projects and applications. ECSS is a cooperative effort of the European Space Agency, national space agencies and European industry associations for the purpose of developing and maintaining common standards.

Requirements in this standard are defined in terms of what shall be accomplished, rather than in terms of how to organize and perform the necessary work. This allows existing organizational structures and methods to be applied where they are effective, and for the structures and methods to evolve as necessary without rewriting the standards.

The formulation of this standard takes into account the existing ISO 9000 family of documents.

This standard has been prepared by the ECSS-E-20-01 Working Group, reviewed by the ECSS Engineering Panel and approved by the ECSS Steering Board.

(This page is intentionally left blank)

Introduction

Single carrier multipaction has well-established theoretical and testing procedures, and the heritage from proven components enables to define testing margin values as requirements for European space missions. Applying the single carrier margin to peak in-phase multi-carrier signals is recognized as excessively onerous in many cases, but the present understanding of multipaction for multicarrier signals is not well enough established for a reduced limit to be specified. For this reason, the margins for the multi-carrier case are stated as recommendations, with a view to their evolving to requirements in the longer term.

(This page is intentionally left blank)

Contents

Figures

Tables

(This page is intentionally left blank)

1

Scope

This standard defines the requirements and recommendations for the design and test of RF components and equipment to achieve acceptable performance with respect to multipaction-free operation in service in space. The standard includes:

- verification planning requirements,
- definition of a route to conform to the requirements,
- design and test margin requirements,
- design and test requirements, and
- informative annexes that provide guidelines on the design and test processes.

This standard is intended to result in the effective design and verification of the multipaction performance of the equipment and consequently in a high confidence in achieving successful product operation.

This standard covers multipaction events occurring in all classes of RF satellite components and equipment at all frequency bands of interest. Operation in single carrier CW and pulse modulated mode are included, as well as multi-carrier operations. This standard does not include breakdown processes caused by collisional processes, such as plasma formation.

This standard is applicable to all space missions.

When viewed in a specific project context, the requirements defined in this standard should be tailored to match the genuine requirements of a particular profile and circumstances of a project.

NOTE Tailoring is a process by which individual requirements of specifications, standards and related documents are evaluated and made applicable to a specific project, by selection and in some exceptional cases, modification of existing or addition of new requirements.
[ECSS-M-00-02A, clause 3]

(This page is intentionally left blank)

2

Normative references

The following normative documents contain provisions which, through reference in this text, constitute provisions of this ECSS Standard. For dated references, subsequent amendments to, or revisions of any of these publications do not apply. However, parties to agreements based on this ECSS Standard are encouraged to investigate the possibility of applying the most recent editions of the normative documents indicated below. For undated references the latest edition of the publication referred to applies.

ECSS-P-001	Glossary of terms
ECSS-E-10-02	Space engineering — Verification
ISO 14644-1:1999	Cleanrooms and associated controlled environments. Classification of air cleanliness

ESCC Basic Specification No. 24900, Issue 1, October 2002, Minimum requirements for controlling environmental contamination of components

ESCC Basic Specification No. 20600, Issue 1, February 2003, Preservation, packaging and despatch of ESCC electronic components

(This page is intentionally left blank)

3

Terms, definitions and abbreviated terms

3.1 Terms and definitions

The following terms and definitions are specific to this standard in the sense that they are complementary or additional to those contained in the ECSS-P-001.

3.1.1
acceptance margin
margin to use for acceptance testing

3.1.2
acceptance stage
verification stage with the objective of demonstrating that the product is free of workmanship defects and integration errors and ready for its intended use

3.1.3
analysis uncertainty
numerical value of the uncertainty associated with an analysis

NOTE In performing analysis, a conservative approach based on pessimistic assumptions is used when assessing threshold powers for the onset of multipaction.

3.1.4
assembly (process)
process of mechanical mating of hardware to obtain a low level configuration after the manufacturing process

(see also ECSS-P-001).

3.1.5
batch acceptance test
test performed on a sample from each batch of flight units to verify that the units conform to the acceptance requirements

NOTE For requirements on the sample size, see 8.3.1a.

3.1.6
design margin
theoretically computed margin between the specified power handling of the component and the result of an analysis after the analysis uncertainty has been subtracted

NOTE As for the analysis uncertainty, the worst case is used.

3.1.7
development test
testing performed during the design and development phase which can supplement the theoretical design activities

3.1.8
gap Voltage
voltage in the critical gap

NOTE The critical gap corresponds to the most critical location in the space RF component where the multipaction can occur.

3.1.9
in-process test
testing performed during the manufacture of flight standard equipment

NOTE It is carried out with the equipment in an unfinished state or on a part or sub assembly that cannot be tested fully when later integrated into the equipment. The tests form part of verification.

3.1.10
integration
process of physically and functionally combining lower level products to obtain a particular functional configuration

NOTE The term product can include hardware, software or both.

3.1.11
measurement uncertainty
uncertainty with which the specified power level is applied to the test item

3.1.12
model philosophy
definition of the optimum number and characteristics of physical models to achieve a high confidence in the product verification with the shortest planning and a suitable weighing of costs and risks

3.1.13
qualification margin
margin between the specified power level and the power level at which a qualification test is performed, taking into account the measurement uncertainty

3.1.14
qualification stage
verification stage with the objective to demonstrate that the design conforms to the applicable requirements including proper margins

3.1.15
qualification test
testing performed on a single flight standard unit to establish that a suitable margin exists in the design and build standard

NOTE Such suitable margin is the qualification margin.

3.1.16
review-of-design
verification method using validation of previous records or evidence of validated design documents, when approved design reports, technical descriptions and engineering drawings unambiguously show that the requirement is conformed to

3.1.17
test margin
margin demonstrated by test

3.1.18
unit acceptance test
testing carried out on each flight standard unit to verify that the unit conforms to the acceptance requirements

3.1.19
verification level
product architectural level at which the relevant verification is performed

3.2 Abbreviated terms

The following abbreviated terms are defined and used within this Standard:

AC/DC	alternating current/direct current
BAT	batch acceptance test
BSE	back-scattered electron
CFRP	carbon-fibre-reinforced plastic
CW	continuous wave
DUT	device under test
ECSS	European Cooperation for Space Standardization
EMC	electromagnetic compatibility
ERS	European remote sensing satellite
ESCC	European Space Components Coordination
FM	flight model
HPA	high power amplifier
IF	intermediate frequency
LNA	low noise amplifier
OMUX	output multiplexer
PIC	particle in cell
PID	process identification document
PIMP	passive intermodulation product
RF	radio frequency
SEE	secondary electron emission
TEM	transverse electromagnetic mode
TWTA	travelling wave tube amplifier
UAT	unit acceptance test
UV	ultraviolet
VSWR	voltage standing wave ratio
WG	wave guide

(This page is intentionally left blank)

4

Verification

4.1 Verification process

a. The process of verification of the component with respect to multipaction performance shall demonstrate conformance to the margin requirements defined in subclauses 4.6.

b. Verification of the component with respect to multipaction shall be performed as part of the overall component verification process specified in ECSS-E-10-02.

NOTE The requirements contained in this standard are in line with those of ECSS-E-10-02, with tailoring specific to multipaction performance verification.

c. Such verification shall be adequately planned for each component

NOTE It can involve a combination of design analyses, inspections, development testing, in-process testing, qualification testing, batch acceptance testing and unit acceptance testing.

4.2 Verification levels

a. Multipaction performance should be verified at the component level.

b. If this is not feasible or practicable, then verification may be performed at the subassembly level.

4.3 Verification plan

4.3.1 Introduction

The verification plan is a key document in establishing and documenting the route to achieve acceptable performance with respect to multipaction. The plan can be a separate document or incorporated into other planning documents.

4.3.2 Generation and updating

a. A verification plan shall be produced in the early part of the design phase.

b. Such a verification plan shall be updated in the light of any unexpected results from analyses or tests.

NOTE The detailed verification plan adopted for any particular project depends on the qualification status of the equipment and on the model philosophy or production philosophy adopted.

4.3.3 Description

a. The verification plan shall present a coherent sequence of activities that are proposed in order to provide adequate evidence that the requirement specifications for the product are achieved for each delivered item.

b. The criteria for successful completion of each of the activities shall be stated and the verification plan shall show how the criteria have been selected, in accordance with this standard, such that meeting of all criteria for each proposed activity results in acceptance of the delivered components with respect to multipaction.

c. The verification plan shall be a configured document and, once accepted by the customer, shall only be modified with the customer's approval.

d. The inputs to the verification plan shall include
   1. this standard,
   2. the component requirements specification,
   3. the proposed design, and
   4. the component qualification status with respect to multipaction performance.

e. The plan shall contain:
   1. A statement of the applicability of existing qualification status.
   2. Description of analyses to be performed (e.g. geometry, excitation, and analysis method), together with a statement of the requested accuracy from analyses, and the minimum design margin shown by the analysis and assumed in the remainder of the plan.
   3. Description of development tests to support the analyses or for other purposes, including, for each test, a description of the test item, the measurements to be made and a description of the intended use of the results.
   4. Inputs to the overall equipment test plan in terms of a list of tests to be performed on each model, including, for each test, the test configuration, type of signal (CW or pulsed), average and maximum power, diagnostic method, sensitivity, environmental conditions, qualification of personnel involved and acceptance criteria.
   5. Inputs to the overall inspection plan, giving details of inspections to be carried out on test items during manufacture, prior to test, after test, at equipment delivery and at the point of integration.
   6. Inputs to any process identification document (PID) that is being used to control similarity between different models or between models in a batch.

f. Subclause e.5. above, referring to the verification plan, should be reviewed after any detailed analysis is completed and any multipaction-critical areas identified for inspection of dimensions, contamination pre-test and damage post-test.

4.4 Verification routes

Verification shall be accomplished by one of the following verification routes:

a. Analysis only, in which case the following requirements shall be met:
   1. there is a proven heritage of similar qualified designs;
   2. the component has a geometry that allows accurate field calculations to be performed with high confidence;
   3. the multipaction-critical areas of the component have commonality with an existing design that has established the correlation between analysis and test.

b. Qualification tests only.

c. Acceptance (batch, or unit or both) tests only.

d. Previously qualified components.

NOTE The relevant margins for all routes are specified in subclause 4.6.

4.5 Classification of component type

a. The classification of component types given in Table 1 shall be used to determine the applicable multipaction margin in accordance with subclause 4.6.

NOTE This subclause defines a classification of component types according to the materials employed in the construction.

b. In case of doubt when determining the classification of any particular component, the type with a higher number shall be assumed.

Table 1: Classification of component type

Type	Characteristics
1	The RF paths are entirely metallic (with known secondary electron emission properties) or are metallic with a non-organic surface treatment that increases the multipaction threshold. Note that this does not preclude the use of coated plastics or CFRP provided that only metal surfaces are subjected to the RF fields. The components are well vented.
2	The RF paths contain or can contain dielectrics or other materials for which the multipaction performance is well defined. The components are well vented.
3	Any components not classified as Type 1 or Type 2.

4.6 Single carrier

4.6.1 General

This subclause states the numerical values of the margins to be used for CW and pulsed systems.

4.6.2 Margins

The margins shown in Table 2 to 4 for the three different component types shall be applied.

NOTE The margin is defined with respect to the peak operating power for the component.

Table 2: Margins applicable to Type 1 components

Route	Analysis margin (dB)	Qualification test margin (dB)	Batch acceptance test margin (dB)	Unit acceptance test margin (dB)
1	8	–	–	–
2	–	6	–	–
3	–	–	4	–
4	–	–	–	3

Table 3: Margins applicable to Type 2 components

Route	Analysis margin (dB)	Qualification test margin (dB)	Batch acceptance test margin (dB)	Unit acceptance test margin (dB)
1	10	–	–	–
2	–	6	–	–
3	–	–	4	–
4	–	–	–	3

Table 4: Margins applicable to Type 3 components

Route	Analysis margin (dB)	Qualification test margin (dB)	Batch acceptance test margin (dB)	Unit acceptance test margin (dB)
1	12	–	–	–
2	–	10	–	–
3	–	–	6	–
4	–	–	–	4

4.6.3 Route to demonstrate conformance

a. The route to demonstrating conformance to CW and pulsed multipaction requirements illustrated in the flow diagram shown in Figure 1 shall be used.

b. The unit shall not be accepted at each stage of the process unless

   1. the relevant margins are satisfied, and
   2. controls in the production process are such that adequate margins are carried through to the final components.

      NOTE The stages in the process are analysis, qualification tests and acceptance tests, where the latter can be either batch or unit tests.

c. If any stage of the process is omitted, then it shall be assumed that the margins are not satisfied and the 'no' route in the flow diagram (see Figure 1) shall be followed.

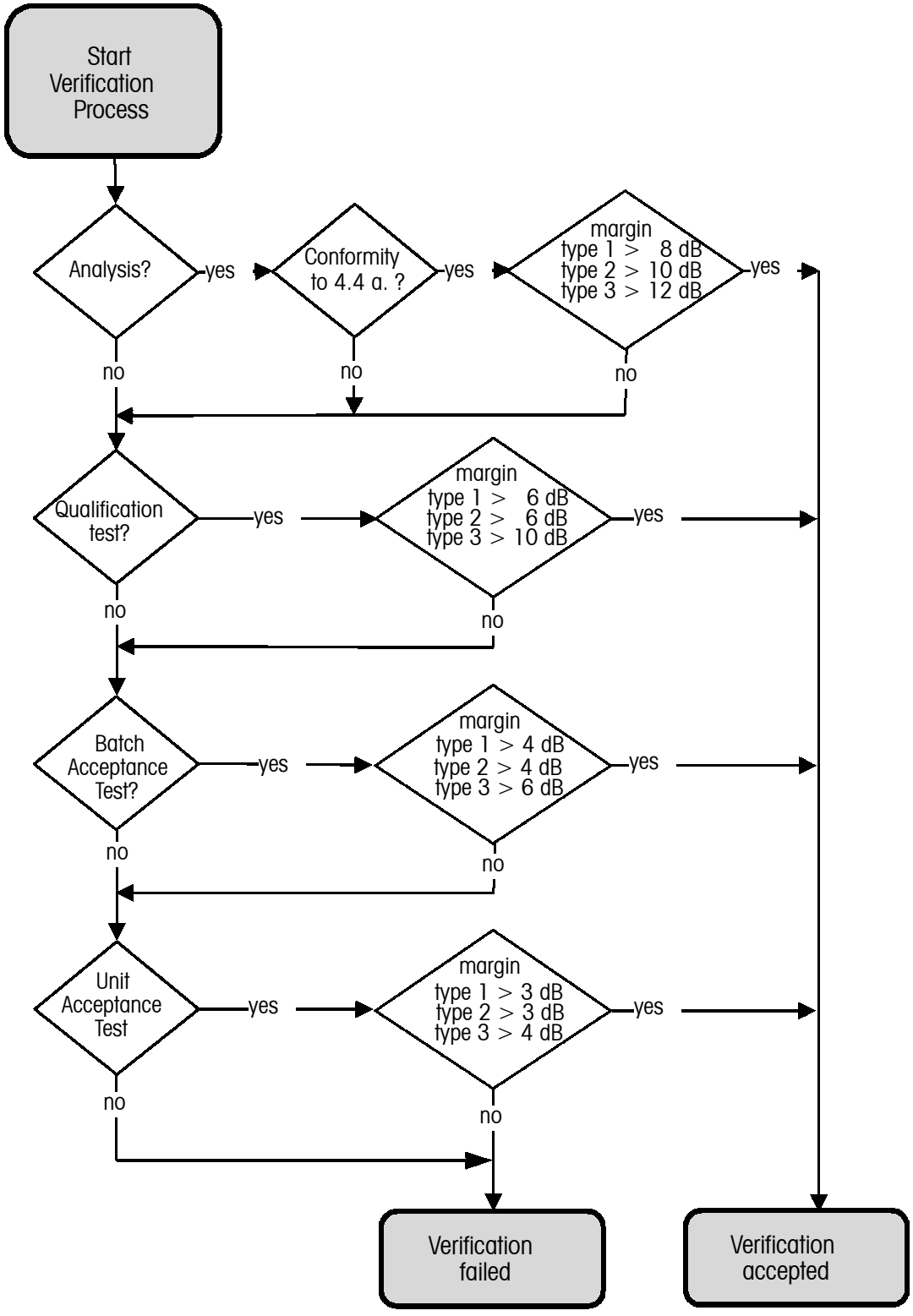

Figure 1: Routes to conformance for single carrier

4.7 Multi-carrier

4.7.1 General

This subclause 4.7 presents recommendations for the verification of multipaction performance under multi-carrier conditions. The purpose of the multi-carrier margin recommendations is to give values which offer low probability for multipaction breakdown without over-designing the parts. These recommendations draw on the results presented in Annex A.

Margins are only quoted for Type 1 components. Margins for component types 2 and 3 are currently under investigation. Verification for two cases is described in the two following sub clauses; the first treats the case of the multipaction threshold above the power of a single carrier CW signal whose power is equal to the peak power of the multi-carrier signal, and the second treats the case of the multipaction threshold below the equivalent single carrier CW peak power. The second case becomes more likely as the number of carriers increases.

Multi-carrier verification follows the procedure used for the single carrier case. Margins are defined with respect to a single carrier signal at the lowest frequency in the multi-carrier signal and at peak power, where the peak corresponds to the worst case in-phase signal power.

4.7.2 Threshold above equivalent CW peak power

a. When the single carrier multipaction threshold is above the peak power, margins shown in Table 5 shall be applied.

b. As for the single carrier case, analysis-only verification shall only be done if the appropriate analysis margin and the requirements listed in subclause 4.6.3 are met.

Table 5: Margins applicable to Type 1 multi-carrier components for single carrier threshold above equivalent CW peak power

Single carrier margin with respect to equivalent peak power				
Route	**Analysis margin** (dB)	**Qualification test margin** (dB)	**Batch acceptance test margin** (dB)	**Unit acceptance test margin** (dB)
1	6	—	—	—
2	—	3	—	—
3	—	—	0	—
4	—	—	—	0

4.7.3 Threshold below equivalent CW peak power

When the single carrier multipaction threshold is below the peak power,

a. margins shown in Table 6 shall be applied;

NOTE 1 In this case, the margins are defined with respect to a power level, P_{20}, corresponding to the peak power of the multi-carrier waveform whose width at the single carrier multipaction threshold is equal to the time taken for the electrons to cross the multipacting region 20 times.

NOTE 2 Informative commentary on the derivation of electron crossing times and P_{20} for multi-carrier waveforms is given in Annex A.

b. a test route should be taken.

Table 6: Margins applicable to Type 1 multi-carrier components for single carrier threshold below equivalent CW peak power

Single and multi-carrier margin with respect to equivalent P_{20}				
Route	**Analysis margin** (dB)	**Qualification test margin** (dB)	**Batch acceptance test margin** (dB)	**Unit acceptance test margin** (dB)
1	6	—	—	—
2	—	6	—	—
3	—	—	5	—
4	—	—	—	4

4.7.4 Route to demonstrate conformance

a. The route to demonstrating conformance under multi-carrier multipaction conditions as illustrated in the flow diagram shown in Figure 2 shall be used.

b. The unit shall not be accepted at each stage of the process unless

   1. the relevant margins are satisfied, and
   2. controls in the production process are such that adequate margins are carried through to the final components.

   NOTE The stages in the process are analysis, qualification tests and acceptance tests, where the latter can be either batch or unit tests.

c. If any stage of the process is omitted, then it shall be assumed that the margins are not satisfied and the 'no' route in the flow diagram (see Figure 2) shall be followed.

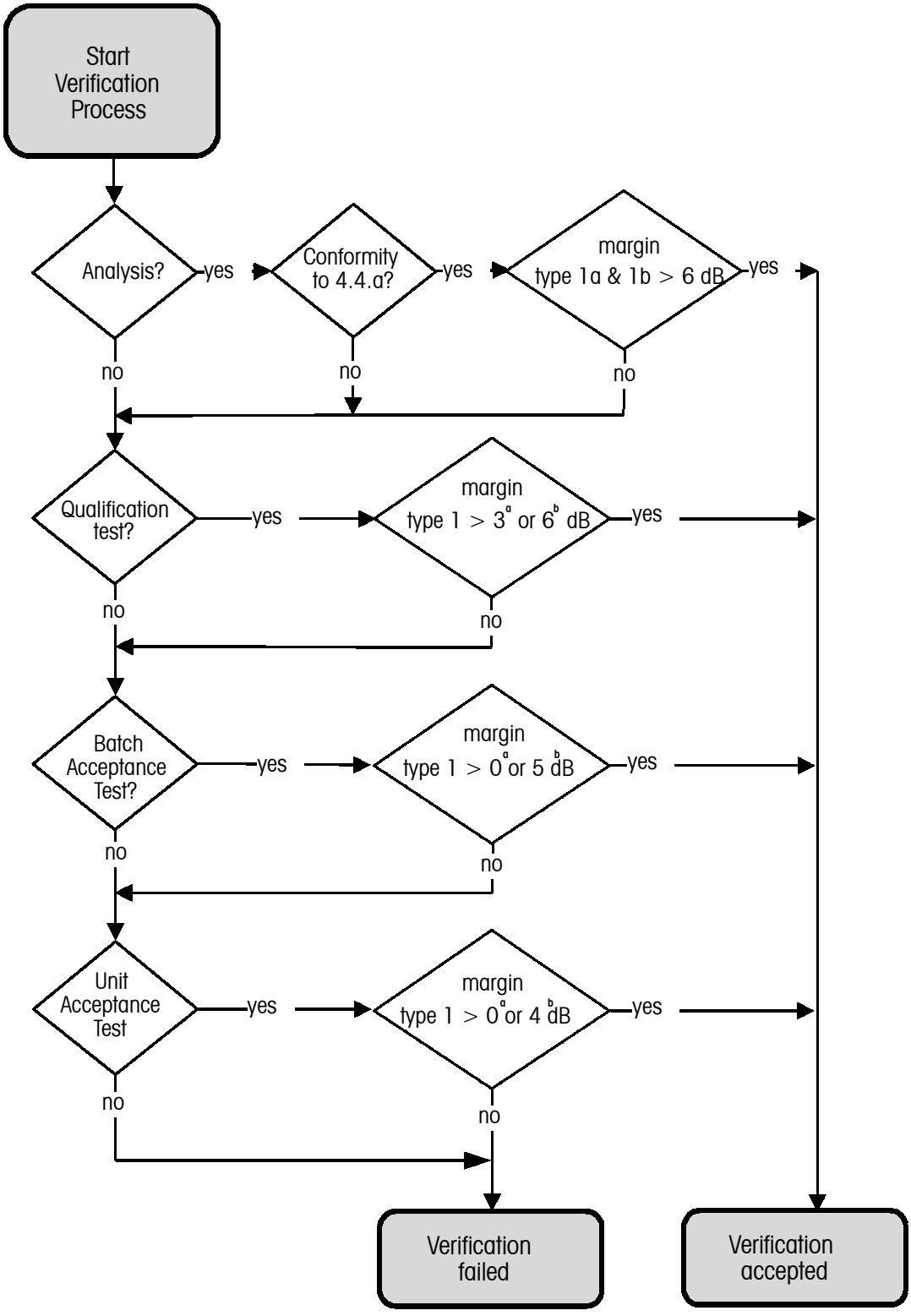

[a] Margin applicable to Type 1 multi-carrier components for single carrier threshold above equivalent CW peak power

[b] Margin applicable to Type 1 multi-carrier components for single carrier threshold below equivalent CW peak power

Figure 2: Routes to conformance for multi-carrier case

5

Design analyses

5.1 General

This clause defines the minimum requirements for performing a satisfactory design analysis with respect to multipaction. These requirements are applicable for all cases where the chosen route to conformance includes analysis. Implementation of such an analysis can vary from sophisticated three-dimensional multipaction simulations to a much simpler estimation process. In all cases, however, a realistic margin (the analysis uncertainty) in the analysis is prescribed to reflect the uncertainty in the analysis method.

5.2 Field analysis

An analysis of the electric field within the component shall be performed.

NOTE This can be accomplished using computer software from measurement on appropriate test pieces or estimated from the appropriate use of equivalent circuit models. A multipaction analysis cannot be performed without a good understanding of the electric fields within the component.

5.3 Critical region identification

a. Any region where high voltages and critical gaps exist shall be identified.

b. The most critical regions shall be located by considering their relevant gap voltages and frequency-gap products.

c. Reference shall be made to the multipaction zones chart defined in Figure 3, which determines the multipaction regions in voltage/frequency-gap space for the relevant materials and geometries.

NOTE For additional information, see Annex A.4.2.6.

d. The multipaction regions referred in c. above shall be subjected to analysis in order to calculate the predicted multipaction threshold.

e. The analysis referred in d. above shall cover all frequencies that are expected for the component in service.

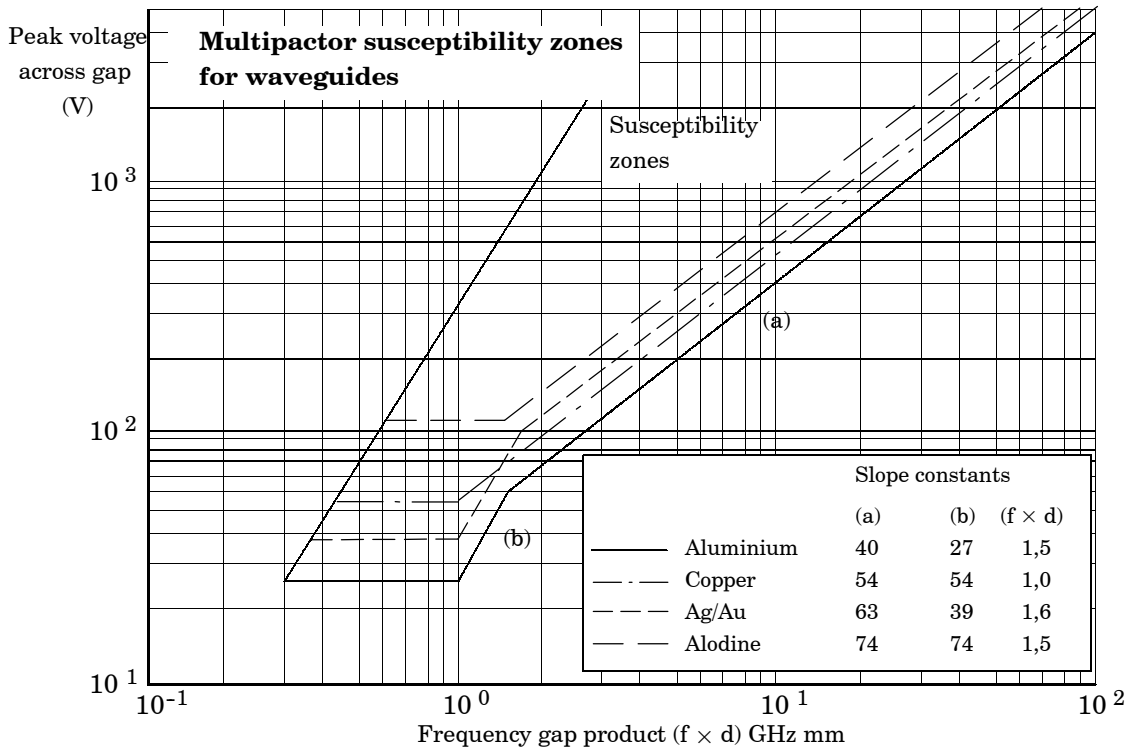

Figure 3: The susceptibility zone boundaries for aluminium, copper, silver, gold and alodine 1200

5.4 Multipaction sensitivity analysis

a. Having located and analysed the critical regions, a sensitivity analysis shall be performed to determine the sensitivity of the multipaction threshold to dimensional variation and changes in material properties.

b. The sensitivity analysis referred to in a. shall then be used to determine the correct degree of mechanical tolerance and process control to impose in cases where acceptance tests are not being performed on all flight units.

5.5 Venting analysis

a. A venting analysis shall be performed to demonstrate that the component is adequately vented.

b. The analysis shall demonstrate that the pressure within the vented component falls to below $1{,}5 \times 10^{-3}$ Pa before RF power is applied, under both testing and in-orbit conditions.

NOTE Annex B illustrates the type of analysis that can be performed.

5.6 Inspection

The outputs from both the multipaction sensitivity analysis and the venting analysis shall be used when determining the inspection requirements to be imposed on the product during all stages of production.

6

Test conditions

6.1 Cleanliness

a. Airborne particulate cleanliness class 8 as per ISO 14644-1, or better conditions, shall be maintained throughout the component assembly, test, delivery and post-delivery phases.

b. In addition, standard clean room practices for handling flight equipment and for general prevention of contamination, agreed with the customer, shall be strictly applied.

c. Protective covers to prevent the ingress of contaminants should be used.

d. Where surfaces are particularly vulnerable to contamination, specific cleanliness control measures should be applied.

NOTE 1 For environmental contamination control of components and for preservation, packaging and dispatch of electronic components, see ESCC Basic Specification No. 24900 and ESCC Basic Specification No. 20600.

NOTE 2 For additional requirements on cleanliness see Annex C.

6.2 Pressure

a. Multipaction testing shall be performed at pressures below $1{,}5 \times 10^{-3}$ Pa in the critical areas of the component.

NOTE This can be achieved by providing an adequate combination of:

* pressure in the vacuum chamber,
* venting design for the component, and
* time for moisture to outgass from the component.

b. A vacuum bake-out should be performed on all components before multipaction testing.

c. The pressure in the vacuum vessel shall be monitored continuously and RF power shall be switched off if any pressure rise occurs and the cause investigated.

6.3 Temperature

a. The thermal dissipation conditions for the DUT during multipaction testing shall be representative of the conditions the DUT is to encounter in its operation.

b. Provided the component can handle increased thermal dissipation, higher input power levels may be used.

c. The thermal dissipation in the DUT caused by the selected multipaction test signal profile (CW, pulsed or multi-carrier) shall be analysed.

d. Any DUT failure due to corona discharge produced by out-gassing build-up caused by thermal dissipation in the DUT shall be differentiated from genuine multipaction discharge.

6.4 Frequencies

a. If the most critical frequencies are not identified by analysis,

   1. non-resonant components should be tested at the lowest frequency of operation, and

   2. components containing resonant features should be tested at the centre frequency and at the band edges.

b. Components designed for multi-carrier use should be subjected to waveforms that seek to simulate as closely as possible the excitation that the component experiences in-orbit.

c. For test purposes, the input excitation referred in b. may be modified as follows, provided that the test conditions are equivalent to or more severe than the operating conditions. The number of carriers may be reduced whilst maintaining the peak power by increasing the power of the individual carriers, with the mean frequency and frequency spread being such as to maintain the multipaction resonance conditions and to ensure that the widths of the power peaks are not smaller than those for the operational frequency plan.

d. The phases of the multi-carrier signals should be adjusted to give worst case conditions at critical gaps in the components.

6.5 Pulse duration

6.5.1 General

Pulsed testing may be applied in the cases of components operating either in CW or in pulsed mode. This subclause 6.5 covers the requirements for the pulse duration.

6.5.2 CW units

a. If pulse testing is used to test units that experience CW excitation in service, the pulse width shall be significantly longer than a characteristic time that is determined by the combination of:

   1. the mean time between seed events within the critical regions of the component;

   2. the time taken for a multipaction event to grow to a sufficiently high level to be detected.

NOTE 1 For units that experience CW excitation in service, pulsed testing can be used to achieve the maximum test power whilst keeping the mean power within the specification of the unit and permitting the use of lower cost test equipment.

NOTE 2 These factors lead to a “dead time”, during which multipaction cannot be detected with a given set of test conditions and test equipment.

b. The dead time shall be determined for the unit under consideration.

c. The pulse width shall be longer than this characteristic time by at least a factor of ten.

6.5.3 Pulse units

The pulse duration used in case of pulse units shall be representative of the longest pulse duration that the unit experiences in service.

6.6 Electron seeding

6.6.1 CW test

An electron seed source need not be used for CW tests.

6.6.2 Pulsed test

a. Electron seeding shall be used in pulsed testing.

b. There shall be an adequate supply of seed electrons in the multipaction-critical regions of the unit.

c. The presence of the supply of seed electrons referred in b. above shall be verified.

6.6.3 Multi-carrier test

There are two types of multipaction event that can occur in a multi-carrier environment:

- Successive peaks in the multi-carrier signal initiate multipaction events in which the electron charge decays completely between signal peaks.
- Successive peaks in the multi-carrier signal initiate multipaction events in which the electron charge fails to decay completely between signal peaks.

The first case can be treated as an extreme of the pulsed case, with electron seeding used and verified.

The second case is similar to CW multipaction with the multipaction event building up over a much longer time-scale than initially expected. An electron seed source need not be used in this case.

Informative commentary on electron seeding is given in Annex D.

In addition, during the peaks the multipaction event can be at such a low level that it sometimes cannot be recorded by transient detection methods.

6.6.4 Seeding sources

a. In all cases where a seeding source is used, the efficacy of the source shall be verified by analysis or experiment.

NOTE The following sources can be used to produce seed electrons:

* radioactive source;
* cold electron emission;
* photoelectric effect;
* electron gun.

b. Owing to the difficulty of the analysis, the verification should be performed experimentally.

c. When the verification is performed experimentally, the following procedure should be used:

1. Fabricate a test piece of representative physical form, wall materials and wall thickness, but with the internal walls of the multipaction-critical region made from copper or silver-plated aluminium, and a theoretical multipaction threshold 3 dB to 6 dB below the peak test power.
2. Activate the intended seeding source.
3. Test the item for multipaction with a CW signal to determine the threshold.
4. Test the item for multipaction with a pulsed signal; decrease the pulse width until it is equal to or below that intended for the subsequent test on the formal item.
5. If consistent multipaction events are recorded and the threshold is constant with changing pulse width, the seeding is proven; if not, reposition the source or increase the seeding rate until these conditions are met.

NOTE The above assumes that the detection method has sufficient sensitivity and response time to detect multipaction during the specified pulse width.

7

Methods of detection

7.1 General

This clause defines the minimum requirements for the detection methods used for multipaction testing. Details of such test methods are included in Annex E.

7.2 Detection methods

a. The detection methods should be selected from the following list:
   1. Global methods:
      (a) Close to carrier noise.
      (b) Phase noise.
      (c) Harmonic noise.
      (d) Microwave nulling.
   2. Local methods:
      (a) Optical.
      (b) Electron probe.

b. At least two detection methods should be present in the test configuration and at least one of them should be a 'global' method.

7.3 Detection method parameters

7.3.1 Sensitivity

a. Each detection method selected shall be shown to have the sensitivity to detect multipaction events.

b. The demonstration specified in a. should be proven using the chosen detection methods and a test piece that shows multipaction at input power levels lower than the peak power to be applied to the deliverable unit.

7.3.2 Rise time

a. Each detection method selected shall be shown to have a sufficiently short rise time to detect multipaction events that are initiated by pulses no longer than those to be applied to the deliverable unit.

b. The demonstration specified in a. should be proven using the chosen detection methods and a test piece that shows multipaction at input power levels lower than the peak power to be applied to the deliverable unit.

8

Test procedures

8.1 Test configurations

The multipaction test configuration used shall conform to the following, as a minimum:

a. The basic configuration for each test shall:
   1. be identified in the test procedure either explicitly or by reference to the test plan;
   2. include the level of detail adequate to enable identification of the calibration or validation approach.

b. The detailed test configuration describing the test set-up for each component shall be included in the test procedure.

c. The test configuration shall include
   1. continuous monitoring of the power applied to the test item, and
   2. a means of accurately calibrating the power monitoring.

d. Appropriate thermal monitoring and control shall be provided for the test item.

e. Continuous pressure monitoring shall be provided within the vacuum vessel.

f. Adequate detection methods shall be provided, and the test configuration shall
   1. enable accurate calibration of the detectors, and
   2. provide an appropriate thermal environment to enable the calibration to be maintained during the test.

g. The test configuration shall be adequately validated, as described in subclause 8.2.

8.2 Test facility validation

A demonstration and validation of the correct functioning of the test configuration shall be performed immediately prior to test and after testing.

NOTE 1 The reason is that, as specified in 8.4.1 a., the criterion for a successful test is a null result, i.e. nothing is detected by the detection system.

NOTE 2 Informative commentary on an appropriate validation method is given in Annex E.4.

8.3 Test execution

8.3.1 General

a. The sample size shall be as defined in the source control drawing.

b. Performance of the multipaction test shall be controlled by a detailed test procedure.

c. After each new test configuration is set up, both the transmitter chain and the detector chain shall be calibrated.

d. For extended or multiple tests with a given configuration, the calibration should be periodically revalidated.

8.3.2 Test procedure

The multipaction test procedure used consists of the following basic steps:

a. The vacuum vessel containing the test item shall be evacuated for a sufficiently long period to enable adequate venting and outgassing of the system.

NOTE For venting and outgassing, see Annex B.

b. The test configuration shall be validated by applying power to multipaction standard and observing the onset of multipaction at the expected power level (see Annex E).

c. The test shall be performed by applying first the lowest test power, and then increasing the power in steps up to the maximum test power, as follows:

1. At each step, the power shall be held constant for the step duration.
2. The maximum test power shall be the power corresponding to the specified test margin.
3. The lowest test power shall be 10 dB below the maximum power, unless a qualification margin is established, in which case the lowest test power level may be increased up to but no higher than 3 dB below the maximum power.
4. The power steps shall be 1 dB until a point 3 dB below the maximum power is reached; at which point the steps shall be reduced to 0,5 dB.
5. The duration of the steps shall be:
   (a) ten minutes in a CW test, for powers below the component rated value;
   (b) five minutes in a CW test, at powers above the component rated power;
   (c) the total aggregate duration of the pulses shall be per (a) and (b) above, not including the interpulse periods, for pulsed testing.

d. During the test

1. the detectors shall be monitored continuously, and
2. actions shall be taken to avoid continuous multipaction discharge in order to prevent component damage.

e. Any detected pressure rise or unacceptable temperature rise shall cause an interruption of the test until satisfactory conditions are restored.

f. On completion of the test, the validation shall be repeated.

g. After reviewing all the test results, the vacuum chamber shall be returned to ambient pressure by purging with dry nitrogen.

h. The calibration of the transmitter chain and detectors shall then be checked to confirm that the calibration is still valid.

8.4 Acceptance criteria

8.4.1 General

a. The acceptance criterion for a successful test shall be that no multipaction is detected during the test at any input power up to the specified peak level.

NOTE It is common experience, however, that as power levels are increased and approach the threshold for the first time that short bursts of multipaction or plasma discharge are detected. The events are not sustained and cannot be repeated. A plausible explanation is that these events are associated with some form of surface conditioning.

b. In cases where multipaction or plasma discharge are detected, as power levels are increased and approach the threshold for the first time:

1. the acceptance criteria shall be that no event occurs after running for one minute and that after that minute the power can be cycled five times between the desired power and 1 dB lower with no detection of multipaction.
2. the test duration should be doubled for that power level.

8.4.2 Multi-carrier test

For multi-carrier tests, the use of sensitive, short rise time detection methods enables recording of occasional isolated transient events, particularly if a high seeding environment is provided.

NOTE At the present time, the acceptance criteria to apply in this case have not been determined.

(This page is intentionally left blank)

Annex A (informative)

Multipaction background

A.1 Physics of multipaction

Multipaction is a well-understood RF vacuum breakdown mechanism whereby there is a resonant growth of free electron space charge between two surfaces. It has been investigated both theoretically and experimentally over many years; for example see references [1] to [7] listed in the Bibliography. Essential ingredients for multipaction are initial seeding electrons, surfaces where the number of secondary electrons per incident electron is greater than unity for the energies of the incident electrons, and electric fields frequencies and surface separation such that the secondary electrons themselves lead to further growth in electron number when they are incident on surfaces.

A typical multipaction event proceeds as follows:

a. Free electrons exist within the RF field region of a component whose dimensions are small compared with the electron mean free path as a result of low pressure within the component.

b. The electric field within the component accelerates the free electrons towards an interior surface.

c. The electrons impact on the surface with appropriate energies to liberate more secondary emission electrons than were incident.

d. The alternating RF field reverses and accelerates the electrons away from surface, reducing the tendency for surface re-absorption of the low energy electrons.

e. Steps c. and d. together are such that the number of free electrons is increased by the interaction with the surfaces.

f. Moving under the influence of the applied RF electric field and the electron-electron mutual repulsion field, the electrons impact on an interior surface of the component after approximately n half-cycles of the RF field. The number n is the ‘order’ of the multipaction event and is almost always odd, signifying a multipaction event between two surfaces, for example the two conductors in a vacuum spaced coaxial cable.

g. Steps c. to f. are now repeated with an increase in the electron population at each impact causing exponential charge growth to occur until a limiting process such as that caused by the electron-electron mutual repulsion causes the electron cloud to saturate.

The basic physical mechanisms that give rise to a multipaction event are therefore: various processes for generating seed electrons, the mutual interactions between electrons and time varying electromagnetic fields, and the surface physics of secondary electron emission. For the case of simple geometries, such as parallel planar or coaxial surfaces, the resonance conditions can be parameterized in terms of the gap voltage and the frequency-gap product, leading to design tools such as the Hatch-Williams diagram. These cases are explored later in this Annex. For space component applications, the relevant bounds are the lowest bound for multipaction to occur, and since the electron-field interaction is almost electrostatic, the bounds given by the Hatch-Williams diagram provide a good initial estimate for more complicated geometries.

A.2 Other physical processes

Electrical breakdown in RF components can arise from surface or volume sources of charge. Under space vacuum conditions, electron population growth through resonant secondary emission at surfaces is the predominant process. If the very low pressure conditions corresponding to the ambient space environment are not met, then collisions between the surface emitted secondary electrons and the residual gas modifies the behaviour, leading to multipaction initiated plasma formation. Under such conditions, the range of voltages over which discharges can occur increases. At higher pressures still, RF breakdown can lead to gas discharge even in the absence of multipaction (see references [8] to [10]). Under space vacuum conditions, plasma formation, RF breakdown and arcing are not the primary processes. However, they can affect test conditions, and it is for this reason that venting and vacuum conditions are addressed in other parts of document (see Annex B).

A.3 RF operating environment

A.3.1 General

This subclause A.3 defines the various RF operating environments that can be experienced by a high power component, namely:

- true CW operation;
- single modulated carrier;
- pulse modulated operation;
- operation with two or more modulated carriers.

At the detail level, there are a large number of schemes, such as modulation schemes and frequency plans. But rather than exploring these, it is more desirable to reduce the number of approaches to the minimum set described in the following subclauses.

A.3.2 CW approach

Conceptually, this is the simplest approach and, also, it has the merit of being the worst case, thus minimizing the risk of in-orbit failure. As the worst case approach, it may be applied in all cases. However, the disadvantage of the approach is that, in multi-carrier cases, it can lead to significant over-design and over-test.

The approach simply involves calculating the peak instantaneous power derived from the modulation scheme, or frequency plan, or both; and then making the assumption that the component is operated in a CW manner at a power level equal to the peak instantaneous power so calculated.

A.3.3 Pulsed approach

In this approach, the component is treated as if it were excited by a pulse-modulated carrier. There are several motivations for adopting a pulsed test approach, which give rise to differences in detail as illustrated below:

a. The pulsed approach is selected because the component is actually intended for operation in a pulse-modulated fashion, for example in a radar system.

b. The pulsed approach is selected for testing in order to achieve the testing peak power levels whilst controlling the mean power level for thermal or other reasons to avoid overstressing the component.

c. The pulsed approach is selected for testing in order to reduce the cost of the high power source.

d. Examples b. and c. above really apply to a hybrid between the CW and pulsed approach in which pulsed testing can be used if it can be demonstrated that the pulsed excitation is no less stringent with respect to multipaction than CW testing.

A.3.4 Multi-carrier approach

The multi-carrier approach is appropriate for components operated in a multi-carrier environment and where the CW approach is rejected either because it can lead to over design or because the implied power levels can make the testing uneconomic or impracticable. For example, a component under 8 multi-carrier unmodulated CW excitation with 100 W per carrier results in testing at 25 600 W input power (assuming a 6 dB margin). Unfortunately, this approach is the most complicated, the least well understood, and so the risks of following this approach are higher.

The essence of the multi-carrier approach is that the component is powered by waveforms that seek to simulate as closely as possible (except for the addition of a margin) the excitation that the component is subjected to in service. Two significant problems arise from this simple concept: firstly there is the question of selecting the actual waveforms to apply from an infinite variety of possible phase conditions of the carriers, and secondly there is the question of the trade-off between sensitivity and resolution of the detection system and the subsequent interpretation of the detected waveforms.

A.3.5 Multi-carrier multipaction thresholds

As the number of carrier frequencies increases, the ratio of peak power to mean power increases, with the consequence that positive margins with respect to the peak power become overly restrictive. However, acceptable multi-carrier multipaction performance can still be realized even though the single carrier margin can be negative. This is the case addressed in this subclause.

To establish verification when margins are negative implies a more detailed analysis in which the duration as well as the magnitude of the multi-carrier power peaks is considered. The procedure makes use of the empirical result that detectable multi-carrier events need signal power levels to be maintained above threshold for a period about 20 gap crossings after initial seeding has taken place (see reference [4]). A verification process based on the same heuristic is as follows:

a. Compute the mean power P_{mean} and peak power P_{peak} from the frequencies and powers of the specified N carriers assuming in-phase or coherent signals.

b. Establish the single carrier multipaction threshold power P_t from the tests, which for the present case is such that $P_{\text{mean}} < P_t < P_{\text{peak}}$.

c. Calculate the (worst case) mode order for the susceptible gaps in the component; in general by performing detailed computations. Detailed calculations for the most used materials are shown in Tables A-1 to A-5.

d. Compute the 20 gap crossing time, τ_{20}, where
τ_{20} = (20 × mode order)/(2 × mean carrier frequency).

e. Compute the power P_{20} that is the maximum power level of the multi-carrier signal for a peak power duration at least equal to the 20 gap crossing time. This value can be obtained using an optimization method which determines the worst case phase between carriers under the conditions defined by the frequency plan and power per carrier proposed for in-flight conditions (see reference [14]).

Table A-1: Worst case mode order for susceptible gaps for gold

Mode	Fd (GHz mm)	V0 (V)	Mode	Fd (GHz mm)	V0 (V)
1	1,3	32,5	51	88,4	3 097,1
3	5,2	182,2	53	91,9	3 218,5
5	8,7	303,6	55	95,3	3 340,0
7	12,1	425,1	57	98,8	3 461,4
9	15,6	546,5	59	102,2	3 582,9
11	19,1	668,0	61	105,7	3 704,3
13	22,5	789,5	63	109,2	3 825,8
15	26,0	910,9	65	112,6	3 947,3
17	29,5	1 032,4	67	116,1	4 068,7
19	32,9	1 153,8	69	119,6	4 190,2
21	36,4	1 275,3	71	123,0	4 311,6
23	39,9	1 396,7	73	126,5	4 433,1
25	43,3	1 518,2	75	130,0	4 554,5
27	46,8	1 639,6	77	133,4	4 676,0
29	50,3	1 761,1	79	136,9	4 797,4
31	53,7	1 882,5	81	140,4	4 918,9
33	57,2	2 004,0	83	143,8	5 040,3
35	60,7	2 125,4	85	147,3	5 161,8
37	64,1	2 246,9	87	150,8	5 283,2
39	67,6	2 368,4	89	154,2	5 404,7
41	71,1	2 489,8	91	157,7	5 526,2
43	74,5	2 611,3	93	161,2	5 647,6
45	78,0	2 732,7	95	164,6	5 769,1
47	81,5	2 854,2	97	168,1	5 890,5
49	84,9	2 975,6	99	171,6	6 012,0

(α_{max}=1,79 E1=150 E2=4000 Slope(a)=64,2 Slope(b)=40,1 Wf1=30,1 Wf2=56,2 see Table A-6)

Table A-2: Worst case mode order for susceptible gaps for silver

Mode	Fd (GHz mm)	V0 (V)	Mode	Fd (GHz mm)	V0 (V)
1	1,0	32,5	51	67,5	3 177,7
3	4,0	186,9	53	70,2	3 302,3
5	6,6	311,5	55	72,8	3 426,9
7	9,3	436,2	57	75,5	3 551,6
9	11,9	560,8	59	78,1	3 676,2
11	14,6	685,4	61	80,8	3 800,8
13	17,2	810,0	63	83,4	3 925,4
15	19,9	934,6	65	86,1	4 050,0
17	22,5	1 059,2	67	88,7	4 174,6
19	25,2	1 183,9	69	91,4	4 299,2
21	27,8	1 308,5	71	94,0	4 423,9
23	30,5	1 433,1	73	96,7	4 548,5
25	33,1	1 557,7	75	99,3	4 673,1
27	35,8	1 682,3	77	102,0	4 797,7
29	38,4	1 806,9	79	104,6	4 922,3
31	41,1	1 931,5	81	107,3	5 046,9
33	43,7	2 056,2	83	109,9	5 171,6
35	46,4	2 180,8	85	112,6	5 296,2
37	49,0	2 305,4	87	115,2	5 420,8
39	51,7	2 430,0	89	117,9	5 545,4
41	54,3	2 554,6	91	120,5	5 670,0
43	56,9	2 679,2	93	123,2	5 794,6
45	59,6	2 803,9	95	125,8	5 919,3
47	62,2	2 928,5	97	128,5	6 043,9
49	64,9	3 053,1	99	131,1	6 168,5

(α_{max}=2,22 E1=30 E2=5000 Slope(a)=62,4 Slope(b)=37,9 Wf1=32,4 Wf2=59,1 see Table A-6)

Table A-3: Worst case mode order for susceptible gaps for aluminium

Mode	Fd (GHz mm)	V0 (V)	Mode	Fd (GHz mm)	V0 (V)
1	2,1	94,3	51	108,2	4 809,8
3	6,4	282,9	53	112,5	4 998,4
5	10,6	471,5	55	116,7	5 187,0
7	14,9	660,2	57	121,0	5 375,6
9	19,1	848,8	59	125,2	5 564,3
11	23,3	1 037,4	61	129,4	5 752,9
13	27,6	1 226,0	63	133,7	5 941,5
15	31,8	1 414,6	65	137,9	6 130,1
17	36,1	1 603,3	67	142,2	6 318,7
19	40,3	1 791,9	69	146,4	6 507,4
21	44,6	1 980,5	71	150,7	6 696,0
23	48,8	2 169,1	73	154,9	6 884,6
25	53,1	2 357,7	75	159,2	7 073,2
27	57,3	2 546,4	77	163,4	7 261,8
29	61,5	2 735,0	79	167,6	7 450,5
31	65,8	2 923,6	81	171,9	7 639,1
33	70,0	3 112,2	83	176,1	7 827,7
35	74,3	3 300,8	85	180,4	8 016,3
37	78,5	3 489,5	87	184,6	8 204,9
39	82,8	3 678,1	89	188,9	8 393,6
41	87,0	3 866,7	91	193,1	8 582,2
43	91,2	4 055,3	93	197,4	8 770,8
45	95,5	4 243,9	95	201,6	8 959,4
47	99,7	4 432,6	97	205,8	9 148,0
49	104,0	4 621,2	99	210,1	9 336,7

(α_{max}=2,98 E1=30 E2=5000 Slope(a)=39,8 Slope(b)=26,6 Wf1=23,3 Wf2=44,7 see Table A-6)

Table A-4: Worst case mode order for susceptible gaps for alodine

Mode	Fd (GHz mm)	V0 (V)	Mode	Fd (GHz mm)	V0 (V)
1	1,2	40,6	51	84,3	3 773,9
3	5,0	222,0	53	87,7	3 921,9
5	8,3	370,0	55	91,0	4 069,9
7	11,6	518,0	57	94,3	4 217,9
9	14,9	666,0	59	97,6	4 365,9
11	18,2	814,0	61	100,9	4 513,8
13	21,5	962,0	63	104,2	4 661,8
15	24,8	1 110,0	65	107,5	4 809,8
17	28,1	1 258,0	67	110,8	4 957,8
19	31,4	1 406,0	69	114,1	5 105,8
21	34,7	1 553,9	71	117,4	5 253,8
23	38,0	1 701,9	73	120,7	5 401,8
25	41,3	1 849,9	75	124,0	5 549,8
27	44,7	1 997,9	77	127,3	5 697,8
29	48,0	2 145,9	79	130,7	5 845,8
31	51,3	2 293,9	81	134,0	5 993,8
33	54,6	2 441,9	83	137,3	6 141,8
35	57,9	2 589,9	85	140,6	6 289,8
37	61,2	2 737,9	87	143,9	6 437,8
39	64,5	2 885,9	89	147,2	6 585,8
41	67,8	3 033,9	91	150,5	6 733,8
43	71,1	3 181,9	93	153,8	6 881,8
45	74,4	3 329,9	95	157,1	7 029,8
47	77,7	3 477,9	97	160,4	7 177,8
49	81,0	3 625,9	99	163,7	7 325,8

(α_{max}=1,83 E1=41 E2=5000 Slope(a)=73,8 Slope(b)=73,8 Wf1=85,6 Wf2=85,6 see Table A-6)

Table A-5: Worst case mode order for susceptible gaps for copper

Mode	Fd (GHz mm)	V0 (V)	Mode	Fd (GHz mm)	V0 (V)
1	1,3	46,8	51	66,5	2 385,0
3	3,9	140,3	53	69,2	2 478,6
5	6,5	233,8	55	71,8	2 572,1
7	9,1	327,4	57	74,4	2 665,6
9	11,7	420,9	59	77,0	2 759,1
11	14,4	514,4	61	79,6	2 852,7
13	17,0	607,9	63	82,2	2 946,2
15	19,6	701,5	65	84,8	3 039,7
17	22,2	795,0	67	87,4	3 133,3
19	24,8	888,5	69	90,0	3 226,8
21	27,4	982,1	71	92,6	3 320,3
23	30,0	1 075,6	73	95,3	3 413,9
25	32,6	1 169,1	75	97,9	3 507,4
27	35,2	1 262,7	77	100,5	3 600,9
29	37,8	1 356,2	79	103,1	3 694,4
31	40,5	1 449,7	81	105,7	3 788,0
33	43,1	1 543,2	83	108,3	3 881,5
35	45,7	1 636,8	85	110,9	3 975,0
37	48,3	1 730,3	87	113,5	4 068,6
39	50,9	1 823,8	89	116,1	4 162,1
41	53,5	1 917,4	91	118,7	4 255,6
43	56,1	2 010,9	93	121,4	4 349,2
45	58,7	2 104,4	95	124,0	4 442,7
47	61,3	2 198,0	97	126,6	4 536,2
49	63,9	2 291,5	99	129,2	4 629,7

(α_{max}=2,25 E1=25 E2=5000 Slope(a)=54,1 Slope(b)=54,1 Wf1=37,1 Wf2=37,1 see Table A-6)

A.4 Parallel plate multipaction

A.4.1 Introduction

As stated in A.1, multipaction is the resonant growth of secondary electron population in RF components. When an electron strikes a surface secondary electrons can be emitted. Secondary electron emission (SEE) has two components: true secondary electrons with relatively low energies and back-scattered electrons (BSE) with larger energies (back-scattered electrons emerge with energies up to the primary electron energy). For each electron impacting a surface, an average

of δ true secondary electrons and an average of η back-scattered electrons are emitted. A fraction ε of the back-scattered electrons are specularly reflected electrons (δ and η are called the true secondary emission scattering coefficient and back-scattered scattering coefficient, respectively).

Each coefficient depends both on the energy of the incident particle and its angle of incidence. Moreover, all coefficients depend on the material and on how that material has been treated. For example, baking in vacuum can significantly reduce SEE because surface impurities are eliminated. For a given material and treatment, a variety of parametrizations for these dependencies are available in the literature (see reference [11]).

The variation of the total secondary emission coefficient $\sigma = \delta + \varepsilon$ with incident particle energy E is unimodal, with a maximum of σ_{max} at $E = E_{max}$ and for many metals $\sigma > 1$ for a range of E as illustrated in Figure A-1. The measured values of these parameters for a copper surface (Cu8A in Table V of reference [11]) are $\sigma_{max} = 2{,}25$, $E_1 = 25$ eV, $E_{max} = 175$ eV and $E_2 = 5\,000$ eV. Table A-6 gives these values for the most used materials.

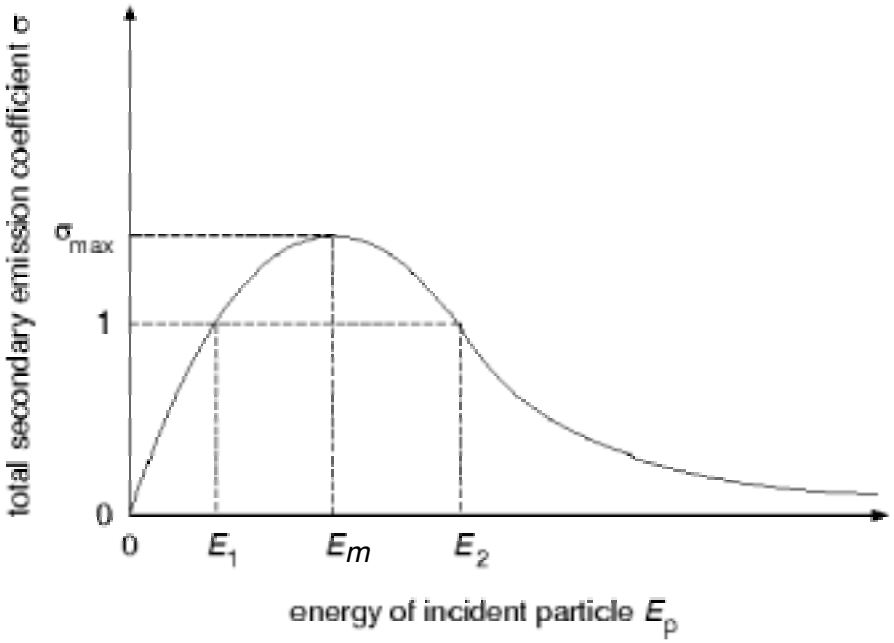

Figure A-1: Total secondary electron emission as a function of energy of the incident electron

The conditions for exponential growth of the true secondary electron population are:

a. the maximum true secondary electron emission coefficient is greater than unity;

b. the incident electron has an energy between E_1 and E_2;

c. the phase of the electric field is such that the secondary electron is not accelerated back into the surface from which it is emitted;

d. the amplitude and phase of the electric field is such that the secondary electron is accelerated towards the opposite conductor and impacts the surface a half-integral number of wave periods after its emission with energy such that it in turn satisfies conditions a. and b.

The Hatch and Williams theory of parallel plate multipaction (see reference [6]) is based on the above conditions and leads to closed regions in voltage - frequency × gap (V–$f \times d$) parameter space for each odd-order resonance. Woode and Petit (see reference [1]) have experimentally tested a number of materials

commonly used in spacecraft components, and have shown that the Hatch and Williams theory is in good agreement with their experiments. Figure A-2, taken from reference [1], shows the zones of susceptibility according to the Hatch and Williams theory (the dashed line, with increasing order at increasing *fd* product), measured threshold points and a design boundary fitted to the data.

NOTE The boundary conditions in this region of the multipaction chart cannot be precisely defined until more experimental verification work is performed.

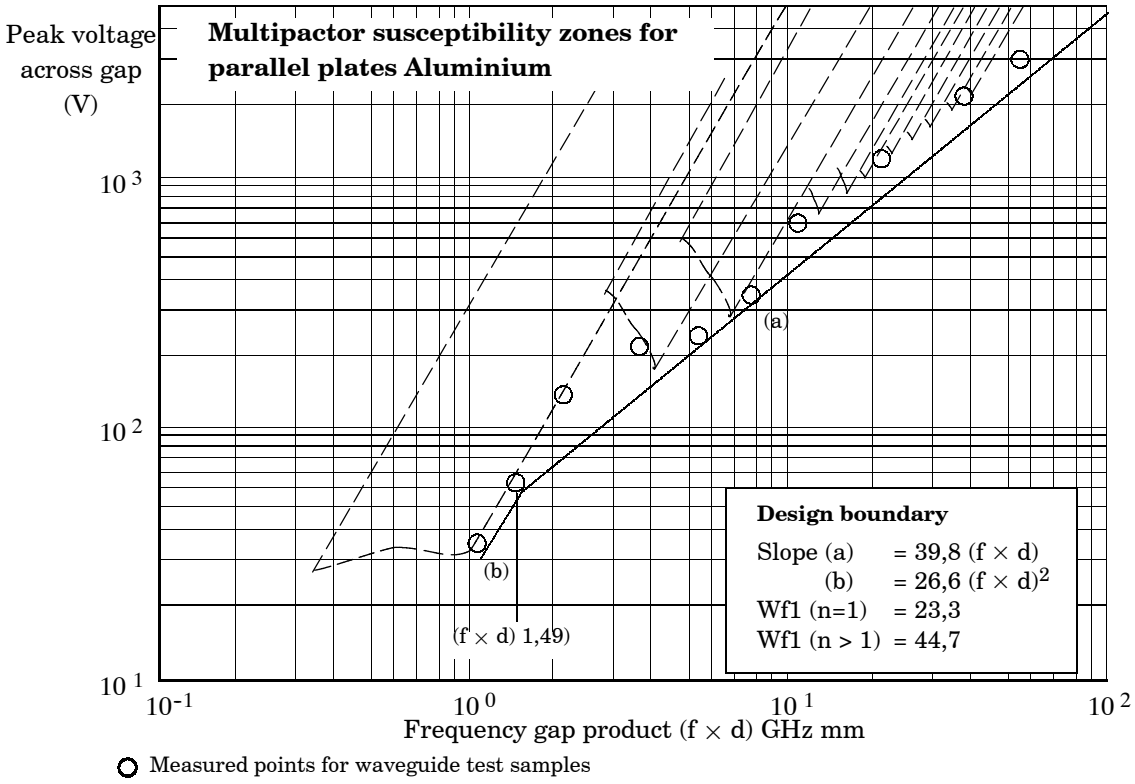

Figure A-2: Multipaction susceptibility zones for parallel plates of aluminum

A.4.2 Woode and Petit results

A.4.2.1 General

The results summarized below are extracted directly from the ESA working paper by Woode and Petit (see reference [1]). Charts of multipaction susceptibility zones as illustrated in Figure A-2 were made for the materials listed below, and a universal susceptibility chart was constructed from the design boundary envelopes for multipaction threshold for the various materials.

A.4.2.2 Materials and surface treatments

The material and coatings were chosen to be as close as possible to common materials used in spacecraft RF payloads. These were:

- Aluminium alloy type Al2024

  This is a general purpose machinable alloy used for the construction of RF payload components. These components are normally plated silver or gold but aluminium is used as a reference for the measurements.

- Alodine 1200

  This is a chromate conversion surface on aluminium, manufactured by a Dutch chemical supplier (Mavom BV). It is used as a protective coating on

aluminium, to be painted or unpainted. It is yellow gold coloured, and the surface thickness is 5×10^2 Å to $7{,}5 \times 10^3$ Å. This coating is used extensively in the construction of spacecraft hardware. It is not normally used for RF components, but has been used for waveguide harnesses.

- Thomson treatment alodine 1200

  The surface treatment is as Alodine 1200, but with a modified preparation schedule. This surface is used on ERS-1 waveguide components.

- Alodine 1500

  This is a chromate conversion surface on aluminium, manufactured by a Dutch chemical supplier (Mavom BV). As a protective coating on aluminium, it is used unpainted and is a colourless film. The coating thickness is 5×10^2 Å.

- Oxygen free copper

  The surface is not normally used for space hardware but is the base material used for silver and gold plating. The machined surfaces were chemically etched before testing.

- Silver plated oxygen free copper

  This is a high purity silver coating, more than 99,9 % pure with no brighteners or stabilisers, coating thickness 7 μm. The typical surface finish is used for high power RF components.

- Gold plated oxygen free copper

  This is a high purity gold coating with more than 99,9 % purity, no added brighteners or stabilisers, coating thickness 7 μm. This surface is sometimes used for high power RF components in space.

A.4.2.3 Observations on results

- It was demonstrated that, when conducting multipaction tests the use of a radioactive or free electron source was a big help in obtaining the true multipaction threshold, especially for the small gap samples.
- With aluminium samples, very little change in multipaction threshold was noted, either with or without a free electron source.
- For samples of silver, gold, copper and alodine, the multipaction threshold was reduced when tested with a free electron source. Gold and copper showed the greatest reduction.
- The multipaction threshold, at a constant $f \times d$, was the highest for alodine, was the lowest for aluminium, and approximately the same for silver, copper and gold.
- The slope of the results for the different materials followed closely the unity slope expected.
- All the results deviated from a straight line in a similar cyclic manner.
- For alodine, the thresholds at $f \times d = 1$ and at $f \times d = 0{,}5$ were equal; for all the other materials, the threshold increased as a function of $(f \times d)^2$.

A.4.2.4 Construction of multipaction susceptibility zone boundaries

Multipaction susceptibility zones for the different materials were constructed from the experimental data. The zone boundaries define the actual multipaction threshold expected, without any margin, except for that of the original measurements made. During component design and testing, allowances were made for the following factors:

- VSWR degradation;
- margin for long-term contamination and handling;
- test measurement errors.

A.4.2.5 Susceptibility zones

In constructing the susceptibility zones from the experimental data, the following assumptions are made:

- A margin of 1 dB has been allowed from the best fit line to the measured points. This allows for inaccuracies in the measurements.
- The change in slope at $n = 1$ was included for Au, Ag and Al. This was not reported before but, according to experience, is correct for waveguides.
- The change in slope constant at $n > 3$ noted for Al and Cu was not included, but for marginal designs it can be included.
- Data for each zone boundary is given:
  - Slope (a) = C $(f \times d)$
  - Slope (b) = C $(f \times d)^2$
  - Change Point $(f \times d)$
- The constants achieved, slope(a) and slope(b) are given in Table A-6.

Table A-6: Constants for the most used materials

Material	α_{max} [a]	E1 [a]	E2 [a]	Em [a]	Slope(a)	Slope(b)	Wf1	Wf2
Gold	1,79	150	4 000	1 000	64,2	40,1	30,1	56,2
Silver	2,22	30	5 000	165	62,4	37,9	32,4	59,1
Aluminium	2,98	30	5 000	805	39,8	26,6	23,3	44,7
Alodine	1,83	41	5 000	180	73,8	73,8	85,6	85,6
Copper	2,25	25	5 000	175	54,1	54,1	37,1	37,1

α_{max} = maximum secondary emission coefficient (see A.4.1)
E1 = lowest incident electron energy at [ρ=1] (see A.4.1)
E2 = highest incident electron energy at [ρ=1] (see A.4.1)
Em = incident electron energy for α_{max} (see A.4.1)
Slope(a) = upper design boundary (see A.4.2.5)
Slope(b) = lower design boundary (see A.4.2.5)
Wf1 and Wf2 are work functions

[a] Data for silver and copper are from [1]. Data for aluminium and alodine are from [13].

A.4.2.6 Universal design curve

To aid presentation of this data, the basic susceptibility zone boundaries for all of the materials were plotted on a common axis, given in Figure 3 (see 5.3 c.). Interpreting below $f \times d = 1$, the constant energy locus used in the theory is discarded as it is not verified by experiment. The constant voltage line used is considered a good estimate of the real situation.

A.5 Coaxial line multipaction

A.5.1 Introduction

Multipacting discharge between coaxial copper electrodes was investigated by Woo (see reference [8]). His work showed that, for coaxial lines of low impedance (under 50Ω), the multipaction susceptibility threshold was similar to that for the parallel plate case. As the impedance of the line was increased, the region of the voltage – frequency × gap parameter space over which multipaction occurred decreased.

More recent work by Arter and Hook (see reference [12]) has used a coaxial line particle-in-cell (PIC) computer simulation code with a Monte-Carlo secondary electron emission module that uses experimentally determined secondary electron emission properties. Their calculations agreed with Wood and Petit's results for copper and reduced to the parallel plate results for low impedance coaxial lines. The results from reference [12] are summarized in A.5.4.

A.5.2 Problem definition

The aim of this work was to predict the multipaction thresholds for coaxial transmission lines. Four coatings with different secondary electron emission (SEE) properties were considered, namely copper (Cu), silver (Ag), aluminium (Al) and alodine (Ald). The SEE properties of a coating can vary appreciably according to how it has been treated. It is desirable to work with the worst case material. Hence for copper and silver, the SEE coefficients used corresponded to the samples labelled Cu8A and Ag3A, respectively, in reference [11]. These are as received values that represent the effects of surface contamination. For aluminium and alodine, the criteria used to obtain the worst case materials are low values of $E1$ and Em, and high σm (using the notation of reference [1]). All the chosen values are listed in Table A-6 (note here that the aluminium sample chosen (Al2A) has different secondary emission properties (reference [13]) from those used by Woode and Petit in the assessment of secondary emission in parallel plate geometry (reference [1]).

The coaxial geometry selected was such that the line impedance, Z, was 50Ω, a value for which experimental results were available. This impedance implies that the inner radius a and outer radius b of the coaxial line are in the ratio $b/a \cong 2{,}3$. In this geometry, twelve threshold calculations were performed for each material at different values of the frequency-gap product $f \times d$ (f is the frequency of the applied TEM wave and the gap $d = b - a$). The $f \times d$ products ranged from 0,7 GHz mm to 30 GHz mm.

A.5.3 Simulations

Simulations were performed using both a two-dimensional (r-z) PIC code and a one-dimensional axi-symmetric PIC code. Both codes used the same Monte-Carlo secondary emission package to model secondary emission, and both codes gave the same results, indicating that magnetic fields and axial drift effects are not important.

A.5.4 Results

The five threshold curves computed are plotted together in Figure A-3 and tabulated in Table A-7. From these, it is clear that aluminium (Al2A) and alodine have very similar multipaction properties. The aluminium materials are superior to silver and copper, which also closely resemble one another. For copper, we have also demonstrated that changing the waveguide gap by an order of magnitude (from d = 1,886 mm to d = 2 cm) has negligible effect, provided the impedance is unchanged.

Table A-7: Critical voltages for multipaction in 50 Ω coaxial lines

	Critical Voltage (V)				
f*×*d	**Silver**	**Alumin-ium**	**Alodine**	**Copper (sample 1)**	**Copper (sample 2)**
1	42,6	49,2	59,0	37,8	37,7
1,4	69,4	74,7	77,6	66,8	66,7
2	120,4	147,6	151,9	114,0	114,6
2,8	196,2	212,4	213,0	190,6	190,3
4	341,7	387,6	391,0	335,2	336,4
5,5	297,3	725,0	721,6	290,9	288,2
7,7	573,7	627,7	622,0	560,6	553,9
10	604,4	1 038,2	1 039,8	594,1	594,0
15	1 330,1	1 452,3	1 446,3	1 032,1	1 010,1
21	1 501,3	2 079,2	2 065,0	1 461,0	1 475,2
30	1 950,4	–	–	1 906,9	1 890,0

NOTE The gap d = 1,886 mm for each material, except for copper sample 1 which represents copper sample 2 walls separated by 2 cm.

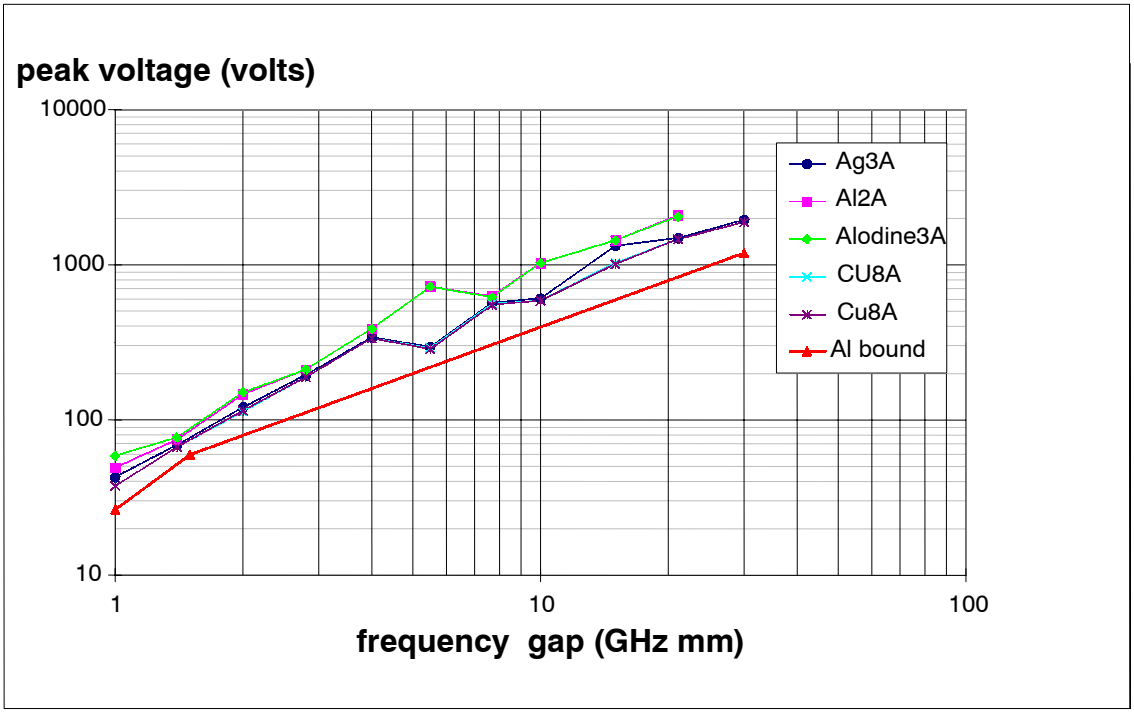

The lower curve labelled 'Al bound' is the parallel plate susceptibility zone boundary for Al2024 from reference [1].

Figure A-3: Multipaction thresholds for all materials studied, plotted in a single graph as labeled.

The similarity of the threshold curves for aluminium and alodine merits some comment. The energy $E1$ at which the secondary emission coefficient σ first becomes greater than unity is normally critical, and since $E1$ = 41 eV for alodine compared to $E1$ = 30 eV for aluminium, it is expected that alodine is superior to aluminium, in agreement with practical experience. However, σ reaches its maximum at a value Emax = 805 eV for the Al2A sample, much higher than the corresponding alodine value of Emax = 180 eV. Thus, σ for the aluminium increases much more slowly for $E > E1$ than σ for the alodine. When the back-scattered fraction η is subtracted from σ to give the true secondary emission coefficient δ for each material, it is found that the δ-curves have almost exactly the same $E1$. It is entirely reasonable to expect that the back-scattered electrons play a negligible role in multipaction (apart from seeding); hence the computed results are consistent with the input data. It is expected that using a more accurate treatment for σ as a function of primary energy can make aluminium appear significantly worse.

At small $f \times d$, different threshold curves are obtained experimentally for different d. The reason for this remains unclear. At large $f \times d$, there is some evidence that the regions of $(V, f \times d)$ space where multipaction occurs become isolated. This makes determining the thresholds very difficult, which argues for more sophisticated search procedures, perhaps involving continuation methods, if detailed two-dimensional calculations of threshold are requested.

It is clear that this computational study is not complete until additional experiments are performed. In addition to validating the numerical model, experimental measurements can help to resolve the issue of the treatment of the SEE properties of aluminium, and can also help to delineate better the multipaction threshold at large values of $f \times d$.

(This page is intentionally left blank)

Annex B (informative)

Component venting

B.1 Introduction

If the ambient background pressure in an RF component is sufficiently high (typically above 10^{-2} Pa), then the multipaction discharge is replaced by a low-pressure gas discharge, where both electrons and ions contribute to free space charge. Low-pressure gas discharges can occur over a wider range of RF voltages than multipaction and therefore adequate component venting is incorporated to ensure that trapped gases do not degrade component performance. To avoid such problems, component venting is designed so that both in testing and under in-orbit conditions pressure is maintained below $1{,}5 \times 10^{-3}$ Pa in the critical areas of the components.

The remainder of this Annex reproduces results on venting guidelines given by Woode and Petit in ESTEC Working Paper 1532 (see reference [1]).

B.2 Discharge dependence on pressure

In previous studies (see reference [15]), it was shown that within a clean environment, multipaction degenerated into a gas discharge at pressures of around 20 Pa and that at all lower pressures multipaction continued unchanged. The conclusion from these early tests was that, provided the pressure was below around 1 Pa, then the only discharges to occur are multipaction.

Further experimentation and component testing showed that this is not always the case. With inadequate venting of waveguide or coaxial components (or cavities) containing for example glues, epoxy compounds, paints, or dielectric materials, discharges can start at much lower levels than otherwise occur. The mechanism for lowering the discharge threshold at these intermediate pressures is usually through localized heating. This can cause:

- Outgassing of contaminants within the potential discharge area building up to a sufficiently high pressure to initiate a gas discharge.
- Outgassing contaminants reducing the surface primary electron energy for σ=l, and hence lowering the multipaction threshold.
- Outgassed contaminants on the surface causing localized high-pressure regions leading to surface discharges.

Therefore, the provision of adequate venting to maintain a low pressure within the component under all operating conditions greatly reduces the possibility of a discharge.

B.3 Test example

Several examples of the reduction in breakdown threshold were observed during tests carried out at ESTEC; one of these is described below (see reference [16]).

This test was carried out on an ERS-1 switching matrix that comprised six waveguide switching circulators containing ferrite, glues and other compounds. The discharge threshold was first measured with the component vented by its own venting holes only; those in the feed waveguides were covered with tape, as they were considered unnecessary. The pressure inside the matrix (which can be monitored) was $2{,}5 \times 10^{-2}$ Pa. In the chamber, it was 5×10^{-4} Pa. Discharges were seen to start at 3,2 kW. These were not multipaction events as demonstrated by the collection of positive ions on the electron probe detector. They caused a reverse polarity output on the oscilloscope and the probe itself to discharge. The discharge was probably a surface discharge caused by the presence of outgassed contaminants.

The same component was then tested with the venting holes uncovered, improving the vacuum to $1{,}5 \times 10^{-3}$ Pa within the matrix. The discharge threshold increased to 10,6 kW and there was a normal multipaction discharge.

From the experience of this and other tests, an internal pressure below 2×10^{-3} Pa can avoid reduction of the discharge threshold. This pressure can be achieved within a reasonable time when in orbit, by sizing the venting holes in accordance with these guidelines.

B.4 Venting dimensions

Sizing of venting holes within payload boxes and equipment so that pressure is released during launch and early orbit, avoiding mechanical stress in the components, is prescribed by current space practices. Conversely, EMC requirements lead to venting holes as small as possible to avoid unnecessary RF leakage. Venting is also usually added as an afterthought with small holes drilled through the waveguide flanges of the components. In the past, with low power components, these design assumptions were found to be sufficient; but for high power components, an end pressure in the cavity or waveguide of around $1{,}5 \times 10^{-3}$ Pa before actual switching on to avoid multipaction and ionization discharges cannot be achieved without the proper sizing of the venting holes. This pressure is achieved only after about 1 to 2 weeks.

The pressure achieved within the component after launch is limited by the ultimate pressure, that is the balancing pressure achieved between the surface outgassing rate of the component inner walls and the pumping conductance of the venting hole. For high power equipment, therefore, the appropriate pumping conductance can be achieved only by a correct design of venting holes, and with the correct number, so as to reach the expected ultimate pressure within the component. In addition, the specific attenuation for EMC purposes cannot be achieved without a correct RF design of the venting hole.

B.5 Venting hole calculations

In the following subclauses, simple equations are given for the calculation of venting hole dimensions. These are backed up by an experiment for the venting of a waveguide cavity. Guidelines are then given for the sizing of venting holes.

B.6 Payload vacuum

The small venting holes are not effective unless the vacuum in the vicinity of the vented component is at least 10 times lower than the pressure within the component. As discussed in [1], the lowest vacuum achievable within the payload volume of a low orbiting spacecraft, like ERS-1, is estimated at 1×10^{-4} Pa. With such a vacuum within the payload cavity, a pressure of 1×10^{-3} Pa can be achieved within the component.

B.7 Venting model used

For calculation of venting hole size a simple cavity mounted in vacuum with a single outgassing hole is used as a model, see Figure B-1.

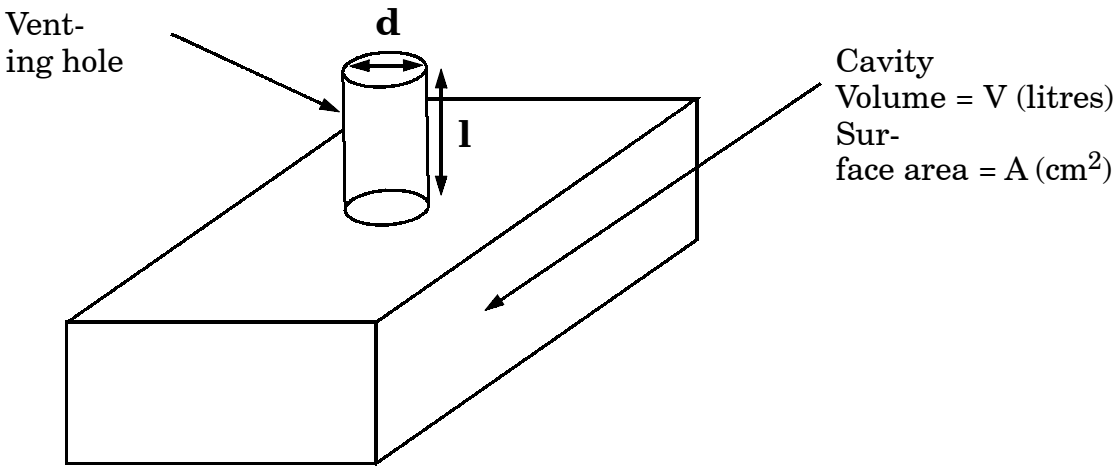

The model has the following parameters:

d = diameter of venting hole, in cm

l = length of venting hole, in cm

Figure B-1: The basic venting model

B.8 Pumping conductance of a venting hole

To calculate the conductance of the venting hole U, the following simplified equation for molecular flow of a gas is used where the mean free path of the gas is greater than the linear dimensions of the venting hole d or l (pressure < 1 Pa). The constants are calculated for air at a temperature of 20 °C.

$$U = \frac{12,1d^3}{(l + 4d/3)} \quad \text{l/s} \qquad \text{(B-1)}$$

The pumping rate of the cavity S_e is dependent on the pumping rate of the vacuum system S.

$$\frac{1}{S_e} = \frac{1}{S} + \frac{1}{U} \quad \text{s/l} \qquad \text{(B-2)}$$

If we assume the available pumping rate $S >> U$, then

$$S_e = U$$

That is, the pumping rate of the cavity is governed solely by the conductance of the venting hole.

The time necessary to pump the cavity from a starting pressure of P_1 to a second pressure P_2 is

$$t = 2,3\frac{V}{S_e}\log\left(\frac{P_1 - P_\infty}{P_2 - P_\infty}\right) \quad \text{s} \qquad \text{(B-3)}$$

Equation (B-3) is only correct when the pressure P_2 is greater than the ultimate pressure in the cavity P_∞.

B.9 Ultimate pressure

The ultimate pressure (P_∞) is achieved after pumping for an infinite time compared to the normal outgassing time calculated from equation (B-3). The ultimate pressure is the equilibrium pressure determined by the outgassing of the internal cavity walls (Q_m per unit area) and the pumping rate of the venting hole S_e, and is given by the equation:

$$P_\infty = \frac{Q_m A}{S_e} \qquad \text{(B-4)}$$

where Q_m is the surface outgassing rate.

The ultimate pressure P_∞ is important, as for small venting holes it defines the final pressure achievable within the cavity. This pressure can exist for many months after launch and is the dominant factor in cavity venting.

The value of Q_m, or the outgassing rate of the cavity walls, is an important parameter. Usually the only way it can be reduced is by heating to drive off absorbed gases. The values of Q_m for some common materials are given in Table B-1. It can be seen that metals generally have a lower outgassing rate than dielectrics, but it is difficult to determine an exact value of Q_m as it varies in published data, presumably due to the actual test conditions.

Table B-1: Outgassing rate for space components used in space applications

Material	Condition	Outgassing rate (Pa m/s)		
		1 hour	10 hours	100 hours
Mild steel	short blasted		8×10^{-3}	
Araldite D			$1{,}3 \times 10^{-3}$	4×10^{-4}
Neoprene		4×10^{-2}	2×10^{-2}	
PVC			$1{,}1 \times 10^{-3}$	$1{,}7 \times 10^{-4}$
Stainless steel		$2{,}7 \times 10^{-4}$	$2{,}7 \times 10^{-3}$	
Aluminium	cleaned in stergene		$1{,}1 \times 10^{-5}$	
Aluminium	anodized		$1{,}3 \times 10^{-4}$	
Brass	cat. washed		4×10^{-4}	
Mylar	outgassed	$2{,}7 \times 10^{-4}$		
Neoprene	as received	$2{,}7 \times 10^{-1}$		

Table B-1: Outgassing rate for space components used in space applications *(continued)*

Material	Condition	Outgassing rate (Pa m/s)		
		1 hour	10 hours	100 hours
Silicone rubber	as received	4×10^{-2}		
Teflon	as received	$6{,}7 \times 10^{-3}$		
PVC	as received	$1{,}2 \times 10^{-3}$		
Textolite	as received	$9{,}3 \times 10^{-3}$		
Mylar	as received	4×10^{-3}		
Stainless steel	polished vap. degr.		$1{,}9 \times 10^{-6}$	
Mild steel		$6{,}7 \times 10^{-4}$	$6{,}7 \times 10^{-5}$	
Nickel plated steel	polished vap. degr.	$6{,}7 \times 10^{-4}$	$1{,}3 \times 10^{-6}$	
Chrome plated steel	polished vap. degr.	$1{,}3 \times 10^{-3}$	$1{,}2 \times 10^{-6}$	
Aluminium	anodized		$1{,}3 \times 10^{-4}$	
Copper		$3{,}1 \times 10^{-3}$		
Nickel		8×10^{-4}		
Molybdenum		$9{,}3 \times 10^{-4}$		
Tantalum		$1{,}2 \times 10^{-3}$		
Zirconium		$1{,}7 \times 10^{-3}$		
Tungsten		$2{,}7 \times 10^{-4}$		
Silver		8×10^{-4}		
Butyl rubber		2×10^{-3}		
Kel F		$5{,}3 \times 10^{-3}$		
Plexiglas	outgassed	$1{,}3 \times 10^{-3}$		
Polyethylene		$3{,}5 \times 10^{-4}$		
Nylon		$1{,}6 \times 10^{-2}$		
Porcelain	glazed	$8{,}7 \times 10^{-3}$		
Steatite		$1{,}2 \times 10^{-4}$		
Epon 828	degreased	$8{,}9 \times 10^{-4}$	$7{,}9 \times 10^{-1}$	$1{,}3 \times 10^{-5}$
Mild steel		$7{,}1 \times 10^{-3}$	$1{,}3 \times 10^{-3}$	$2{,}5 \times 10^{-6}$
Aluminium		$2{,}3 \times 10^{-4}$	$3{,}6 \times 10^{-5}$	$6{,}1 \times 10^{-6}$
Teflon		$6{,}1 \times 10^{-4}$	$2{,}8 \times 10^{-4}$	$1{,}2 \times 10^{-2}$
Copper 450 °C	none	$2{,}1 \times 10^{-3}$		

Table B-1: Outgassing rate for space components used in space applications *(continued)*

Material	Condition	Outgassing rate (Pa m/s)		
		1 hour	10 hours	100 hours
Copper 450 °C	degreased, pickled	$3,5 \times 10^{-4}$		
Copper 450 °C	degreased	$1,9 \times 10^{-3}$		
Aluminium 450 °C	none	$1,7 \times 10^{-3}$		
Stainless steel 450 °C		$8,5 \times 10^{-4}$		
Stainless steel 450 °C	degreased	$5,3 \times 10^{-4}$		
Stainless steel 450 °C	annealed	$7,1 \times 10^{-3}$		
Mild steel 450 °C	none	$5,6 \times 10^{-4}$		
Mild steel 450 °C	degreased	$4,8 \times 10^{-4}$		
Stainless steel 400 °C	none	1×10^{-6}		$1,5 \times 10^{-7}$
Stainless steel 400 °C		$1,6 \times 10^{-3}$		
Stainless steel 400 °C	baked 24 h 200 °C		2×10^{-7}	
Stainless steel 400 °C	baked 12 h 400 °C		$1,2 \times 10^{-8}$	
Stainless steel 400°C			$1,9 \times 10^{-6}$	
Al 6061-T6			$3,3 \times 10^{-6}$	
Al 6061-T6 200 °C			6×10^{-6}	
Al 6061-T6	baked 13,5 h 200 °C		$4,9 \times 10^{-7}$	
Al 6061-T6 300 °C			$1,9 \times 10^{-5}$	
Al 6061-T6	baked 15 h 300 °C		$2,1 \times 10^{-7}$	
Mild steel	none		$2,5 \times 10^{-6}$	
Mild steel	none			$5,3 \times 10^{-7}$
Mild steel 200 °C			$8,8 \times 10^{-6}$	
Mild steel	baked 15 h 200 °C			$5,7 \times 10^{-8}$
Mild steel 400 °C			$1,3 \times 10^{-5}$	
Mild steel	baked 15 h 400 °C			
Stainless steel	degreased	$1,3 \times 10^{-13}$	$2,7 \times 10^{-13}$	$1,2 \times 10^{-7}$
Stainless steel	untreated	$2,3 \times 10^{-4}$		

B.10 Venting experiment

An experiment was carried out using a closed waveguide cavity; this included two venting holes and a means of measuring the internal pressure. The whole cavity was placed within a vacuum chamber and the internal and external pressures were monitored. Some findings of the experiment are summarized below.

The venting time of this cavity, to achieve a pressure of 10^{-3} Pa, was very much longer than predicted by the simple venting equation (B-3) (17 s). This demonstrated that the vacuum obtained was limited to the ultimate pressure P_∞ defined in equation (B-4).

The slowly reducing pressure within the cavity was seen to depend on the outgassing rate Q_m of the cavity walls. Although reducing the pressure to 4×10^{-3} Pa took 1 day, extrapolating the slope of this decay showed that achieving a pressure of 10^{-3} Pa can take 6 weeks.

B.11 Venting guidelines

Based on experience a pressure within the component no greater than $1{,}5 \times 10^{-3}$ Pa after a reasonable time in orbit, as justified in B.2, cannot be achieved without a good venting for all high power components and waveguides.

The steps to calculate venting holes are as follows:

- Choose the dimensions of venting hole considering EMC requirements and RF leakage.
- Calculate the hole pumping conductance 'U' using equation (B-1).
- Choose the minimum number of holes to vent the component, applying equation (B-4) to obtain an ultimate pressure P_∞ of $1{,}5 \times 10^{-3}$ Pa.

For components like waveguide runs, it is good practice to distribute the venting holes along the length with a separation dependent on the distributed volume of the waveguide.

All the above calculations are applicable if the outside of venting holes is close to free space vacuum. The calculation in the case of components enclosed within a vented box is beyond the scope of this Annex.

(This page is intentionally left blank)

Annex C (normative)

Cleaning, handling, storage and contamination

C.1 Generic processes

C.1.1 Introduction

The presence of contaminants within a satellite RF system can contribute significantly to discharges that take place within that system. Discharge can either be multipaction with a lower threshold power than expected or a local ionization discharge from plasma formation at surfaces containing the contaminants.

C.1.2 Cleaning and handling of critical components

To maintain the integrity of the multipaction tests during in-orbit operation, the following specifications on control of environment contamination of components and on the preservation, packaging and dispatch of electronic components shall be applied:

a. ESCC Basic Specification No. 24900.

b. ESCC Basic Specification No. 20600.

NOTE These documents do not address specific multipaction susceptibility issues. For example, it was shown during the ERS satellite test programme and in other tests that significant degradation in multipaction can arise from plastic storage bags.

C.2 Cleaning, handling and storage

C.2.1 Introduction

Multipaction performance cannot be optimized and maintained unless components are cleaned thoroughly before assembly, and handling and storage, through all the stages, are carried out with the utmost care. As explained in C.1.2, multipaction is not specifically covered there, and therefore this subclause C.2, covering specific multipaction issues, is applicable in addition to C.1.2.

The presence of contaminants within a satellite high power RF system can contribute in a significant way to discharges that take place within that system. Discharges can be either multipaction, with (usually) a lower threshold power than predicted, or if severe, can degrade into a local ionization discharge. This discharge is observed as a plasma on the surface containing the contaminant and

the power absorbed is usually greater than for a multipaction discharge, with a consequent increase in temperature and component loss.

When contamination is present, multipaction usually occurs at a lower threshold due to the reduction of the primary electron energy E_1 to achieve a secondary emission coefficient of $\sigma=1$. The reason is that contaminants usually have a greater yield of secondary electrons max than that of the base metal.

One not so well known problem due to contaminants within a high power system is that they can migrate throughout the interconnecting waveguide runs to more critical areas, thus reducing its discharge threshold significantly.

C.2.2 Cleaning and handling of critical components

C.2.2.1

For the cleaning and assembly of multipaction-critical components the following procedure should be followed:

a. Initial cleaning (e.g. new components, screws and shims):
   1. Scrub in Isopropyl Alcohol with cotton buds or lint free tissue.
   2. Ultrasonic clean in Isopropyl Alcohol, in 5 minute cycles (minimum).

      NOTE The number of stages is normally two, but depends on the cleanliness achieved.

b. Cleaning cycles before assembly:
   1. For non crystalline structures, the following ultrasonic cleaning should be used:
      (a) Immerse parts in a warm Isopropyl Alcohol ultrasonic bath for a minimum time of 5 min.
      (b) Repeat ultrasonic cleaning in warm Isopropyl Alcohol bath.
   2. For crystalline structures, or if the ultrasonic cleaning specified in a.2. above is not used, wipe clean the critical areas with Isopropyl Alcohol on cotton buds.

      NOTE Ultrasonic baths can damage some component materials. Crystalline structures are particularly susceptible to fracturing with such treatment. Cleaning agents can have an effect on the organic compounds such as glues and epoxy, as they can be dissolved along with the unwanted contaminant.

c. Assembly:
   1. Transport to assembly area wrapped in lint free tissue.
   2. Blow dry with dry nitrogen to ensure complete removal by evaporation of the solvents.
   3. Assemble using cotton gloves.
   4. Blow with dry nitrogen to remove dust.

C.2.2.2

Glycol Ether based cleaners shall not be used.

C.2.3 Storage of components

C.2.3.1 General

In the light of results obtained during the ERS satellite test programme and other tests where significant degradation in multipaction occurred due to contamination, the methods used for long term component storage are applicable in the present case.

C.2.3.2 Handling

a. External protection

1. Storage should be performed by using hard plastic boxes rather than plastic bags.
2. If hard plastic boxes are used, they should be cleaned before use with a solvent, such as Isopropyl Alcohol.
3. If plastic bags are used, direct contact of the plastic with the component shall be prevented.
4. To prevent the direct contact of the plastic with the component in the case specified in point a.3. above, the component should be well wrapped with lint free tissue.

b. Inert gas

With the component in the bag or box, this should be filled with an inert gas such as dry nitrogen so as to exclude the normal atmosphere.

c. Storage environment

The protected component should then be kept in a stable environment, as specified in ESCC Basic Specification No. 24900.

C.3 Contaminants

C.3.1 The effect of contaminants on the multipaction threshold

During the ERS-2 programme, a measurement campaign was undertaken using standard test samples. Controlled amounts of contamination were applied to these to try and obtain more quantitative results for its effects on the multipaction threshold. The contaminants used were from volatile substances such as glue and potting compounds used in the space industry and present during normal handling and storage.

The test samples used were regular alodine treated aluminium, 1 mm or 2 mm reduced height waveguide sections. The multipaction threshold was monitored both prior to the contaminant being added and again after the contaminant had been removed. The conclusions from these tests are presented in this subclause C.3. For a more detailed description of the tests and test methods used, refer to subclause 4.2.0 in reference [1].

C.3.2 Contamination measurement (wipe test)

The wipe test is an ESA standard for the detection of organic contamination on surfaces (see reference [17]). There are several variations on this method, but typically:

- The sample is washed in chloroform which has a very low non-volatile residue level.
- This solution is evaporated slowly at room temperature.
- The last remaining drops of solution are transferred to an infrared transparent plate.
- The level of contaminants present on the plate is established by infrared spectroscopy.

The sensitivity of the method is about 2×10^{-8} g/cm^2.

In the cases of contamination described below, especially due to the polythene bag lubricant, it was not possible to quantify the surface contaminant present on the multipacting surface using this method. Therefore such methods are not suitable for the determination of the presence of contamination.

The only reliable method known for the detection of all contaminants that can influence multipaction is the multipaction test itself.

C.3.3 Summary of tests made and the results

The contaminants chosen are from compounds used regularly during the construction of space hardware, and through incorrect handling or storage. These were:

- Potting compound

  An example is Solithane 113-30. This is a potting compound used extensively on electronic component and circuits in space. This is also the binder in polyurethane paint used for painting space equipment. The contamination level used was 1×10^{-6} g/cm^2. For space hardware, a contamination level of 1×10^{-7} g/cm^2 is considered acceptable.

  With this contaminant, a slight increase in breakdown threshold was observed but this was within the measurement error of the test equipment of ± 1 dB. On a control sample, this contaminant was seen to completely evaporate within 3 days.

- Epoxy glues

  An example is 3M scotchweld. This is a space-qualified epoxy glue used extensively in the construction of space hardware. It is used as the glue in some high power isolators. There was a significant reduction in multipaction threshold, equivalent to 2,2 dB; greater than the measurement error.

- PTFE (Polytetrafluoroethylene) spray

  An example is Eriflon PTFE. Used as a low friction coating, it is also used as a release agent in the construction of carbon fibre waveguide components. No significant change in discharge occurred although the surfaces were very well covered with a PTFE film.

- Heat sink compound

  An example is Dow Corning Q5-8003. This is space-qualified material and has a low volatility. It is based on silicon compounds filled with heat conductive metal oxides. The multipaction threshold was seen to be reduced by about 2,2 dB from the standard test sample; this did improve slightly with conditioning.

- Dust in critical area from incorrect storage or poor clean room facilities (2 measurements)

  With dust contamination of 145 μg/g there was no significant decrease in multipaction threshold. With the thicker dust sample of 600 μg/g, this made a significant reduction in multipacting threshold of 2 dB, which is greater than the measurement error margin.

- Fingerprints from handling without cotton gloves.

  A slight degradation was noted and discharges were of a regular nature. A drop in threshold of 1,4 dB was on the borderline of measurement error. The contaminant is naturally occurring from oils in the skin and perspiration. Clearly with contaminated fingers this is significantly different.

- Polythene bag lubricant

  These bags contain an organic lubricant called Oleamide, which is added to the polymer at a concentration of 700 μg/g when manufactured. This agent diffuses to the surfaces of the polythene to form a low friction film which is replenished as it is worn away, thus preventing the inner surfaces from sticking together.

  Direct contact of the bag surface with the multipacting surfaces had the greatest effect: up to 4 dB reduction in observer multipaction threshold. The most significant effect was the hysteresis and variability of the discharge; it changed in a random way with usually a large hysteresis between the discharge starting and finishing.

C.3.4 Summary conclusions to the tests

It is clear from all of these results that discharges are difficult to avoid if there is not absolute cleanliness of all the components within a high power system. The use in the production of components of the same standards of cleanliness used for hard vacuum devices, such as TWTAs, can avoid problems during the components' lifetimes.

The following comments can be made:

- The Oleamide contamination from the plastic bags was the most damaging of all the contaminants tested and so this test was repeated many times to check its validity.
- Once it had been initiated, the discharge had a characteristic hysteresis or changeability; this suggests that the initial discharge caused the contamination to migrate.
- By continually allowing a discharge at the higher power levels, some conditioning or cleaning up occurred, but the threshold did not increase to its pre-contaminated value.
- With such contaminated samples, it was not feasible to measure the amount of contamination present using the standard technique described above. For the Oleamide, the amount of contaminant which reduces the multipaction threshold is clearly very small and is probably only a few molecular layers thick.
- The most significant changes occurring were from laboratory contamination, with a reduction in multipaction threshold of up to 4 dB. These are degradations that are not normally expected. Handling and dust can go unnoticed and a plastic bag is usually used to protect a component from contamination, not to cause it.
- Compounds such as epoxy or heat sink compounds within the multipaction discharge zone are not appropriate if multipaction is a major concern. The use of these compounds reduces the effective multipaction threshold to that of untreated aluminium, or below. It was also observed that components from the epoxy showed signs of migration under the action of a discharge.
- When discharges occur at a lower power level due to contamination, the assumption that they are going to clean up during operation is wrong. It can be that the time over which the component can withstand such discharges, without damage, is shorter than the duration of the conditioning cleaning process. This is because of the localized heating that takes place (see case 1).

(This page is intentionally left blank)

Annex D (normative)

Electron seeding

D.1 Introduction

The importance of electron seeding depends upon the nature of the test. Four separate cases are considered below, followed by a description of various types of seeding source.

D.2 CW test

A specific electron seed source needs not be provided for CW testing.

NOTE However, the use of such a source is a common practice.

D.3 Pulsed test

For pulsed testing

a. a source of seed electrons shall be used, and

b. it shall be verified that the source specified in a. provides an adequate supply of seed electrons.

D.4 Multi-carrier test

D.4.1 General

The content of the next two subclauses is preliminary and not based on the same degree of experience and understanding as the CW and pulsed cases.

D.4.2 Generic multi-carrier test

In some respects a multi-carrier test is an extreme case of a pulsed test in that if the threshold power is exceeded at all, it is exceeded for very short times as carriers go through conditions of in-phase addition. This tends to suggest that multi-carrier tests cannot be performed without an adequate seeding and very fast detectors. However, there are reports of reliable multipaction detection in multi-carrier tests without the use of a seeding source, and further that adding a seeding source makes no difference.

There is a simple explanation to reconcile these apparently contradictory statements. Multi-carrier excitation differs from pulsed testing in that the time-scale between in phase carrier addition is also short and that lower levels of RF field are applied at all times. It was observed in computer simulations that with many types of excitations, particularly in components whose dimensions are such

that the onset of multipaction expected is at a high order multipaction mode, successive excursions above threshold generate more electrons than are reabsorbed during the longer periods between the peaks when the power is below threshold. In this way, a multipaction event builds up over a much longer time-scale than initially expected. Such events can indeed be insensitive to seeding and can best be detected by detectors optimized for sensitivity rather than time resolution.

The type of multipaction described above has much in common with CW multipaction events: it is a phenomenon to avoid in-orbit and the acceptance criteria for such a test are similar to the CW case in that the acceptance criterion is that no such multipaction is detected during the test. This leaves the question of much shorter single transient events that have a time-scale comparable with the duration of a single multi-carrier envelope peak; this is the subject of the next clause.

D.4.3 Multi-carrier test with transient detection

In many cases, components can be operated in a multi-carrier environment with transient peak powers significantly above the multipaction threshold. Particularly if no seeding is present, the component can operate for many hours with nothing being detected by fast rise time detectors, provided that the conditions for the long-term charge buildup described above do not exist. Each transient peak above threshold is effectively isolated from the next peak because any charge cloud created during a transient decays before the next transient peak. Occasionally, it can happen that a seed event occurs at the very start of a high power peak and there is sufficient buildup of charge for the event to be detected. Such isolated transient events exist theoretically and were detected experimentally, but only with some difficulty.

It is believed that, at present, no supplier of high power equipment is performing tests capable of detecting such events, but the justification for not performing such tests is not clear. A route to determine the applicability of these tests is to consider the following questions:

- How often are such events going to occur in orbit?

  This question can only be answered by obtaining information on the effective seed rate in orbit, which is presently unknown.

- Do individual events impact on system performance?

  This question can be assessed either theoretically by computer simulation or empirically by performing appropriate pulsed tests with a pulse duration selected to be representative of the duration of typical high power peaks plus an allowance for the mean time between seed events and the characteristics of the detector. The results of such testing can then be used to model the impact on system performance.

- Do multiple events impact on system performance?

  This depends on the answer to question 1, but a meaningful assessment to determine the rate of occurrence of single events to impact upon system performance can be done to determine whether the implied seed rate is at all feasible.

- Do individual events cause component damage?

  This issue can be addressed by means of an analysis of the worst case electron bombardment and then making development test measurements on representative surfaces using an electron gun to simulate the event.

- Do multiple events cause component damage?

  An approach similar to that described above can be appropriate, or alternatively, the component can be subjected to multipaction testing for many hours applying a high seed rate and then inspected for damage.

Unfortunately, simple generic answers to these questions are not available at the present time.

D.5 Types of seeding source

D.5.1 General

The following seed sources may be used:

a. Radioactive β source, which produces high-energy electrons that, after impacting with metal surfaces or propagation though metallic walls, yield a supply of low energy seed electrons. Determining the seed rate involves measuring the source activity and then computing the low energy yield rate.

b. UV light source, which produces electrons by the photoemission mechanism. UV light illuminating the component's inside walls at places close to the critical gap can be used as a seeding source.

c. An electron gun, which produces a known beam of electrons where both the energy and flux can be characterized.

d. A charged wire probe, which produces electrons by the point discharge mechanism.

D.5.2 Seeding inside the component

In the seeding method specified in D.5.1 b. to d., the seeding source shall have access inside the component under test.

(This page is intentionally left blank)

Annex E (informative)

Test methods

E.1 Introduction

This Annex briefly describes the test configurations that have been used for multipaction testing. This information was supplied by members of the working group established to produce recommendations for equipment multipaction design and test; contributions are attributed in each case. The last subclause of this Annex specifically addresses the techniques used for the detection of transient multipaction, as can be produced in a multi-carrier environment.

The test methods included in this Annex rely on the effect that multipaction has the following characteristics:

- phase noise;
- return loss;
- harmonic noise.

The above are global methods in the sense that the effects can be detected at convenient locations remote from the multipacting region. In addition to these, two local methods of detection, namely optical and electron density, are considered in the final clause of this Annex.

E.2 General test methods

E.2.1 Close to carrier noise

E.2.1.1 COM DEV Europe contribution (close to carrier noise floor detection method)

Below is a description of the basic test site used by COM DEV to carry out multipaction testing, along with the minimum conditions for carrying out a test. Note that these are minimum conditions, which are only used in the absence of any overriding information in the test procedure, being the specific test procedure tightening these conditions specified on a case by case basis by the engineering design team.

The generic test site shown in Figure E-1 has the following key parameters:

- The spacing between carrier and detection frequencies is set between 100 MHz and 150 MHz.

- The level of sensitivity of the LNA plus spectrum analyser is set to -120 dBm. It can be reduced, but not beyond a minimum value of -100 dBm. The spectrum analyser is set to a 1,0 MHz span and 1,0 kHz bandwidth.
- The isolation provided by the filters between the TWTA and the LNA is 100 dB as a minimum.

Each test site is calibrated before use. This includes a check that the site is able to detect multipaction, and that the site is multipaction-free up to its maximum specified power. At COM DEV Europe this is carried out monthly on all standard test sites.

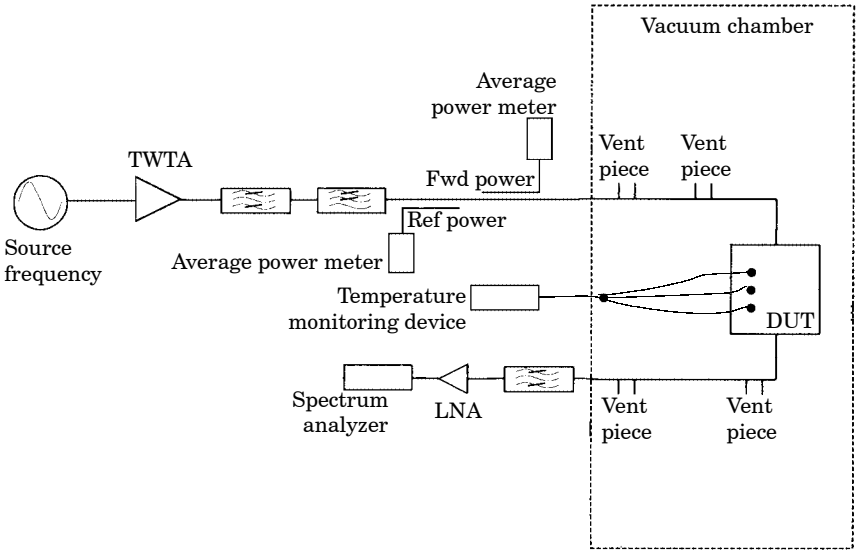

Figure E-1: Generic close to carrier noise multipaction test site

The key factors of the test procedure are:

- the method can be used in either CW or pulsed mode, with single or multi-carrier signals;
- the minimum pulse duration for a pulsed test is 2 μs;
- the minimum soak time in hard vacuum (<1,33 × 10^{-3} Pa) is one hour;
- test is suspended if the DUT reaches 120 °C;
- the power is left on for a minimum of 5 min at each level and 60 min at the final level;
- for single carrier tests the peak power level increments, in Watts, are typically:
  - up to 1 000: 10, 100, 500, 1 000;
  - from 1 000 on, the increment is 1 000: 1 000, 2 000, 3 000, ...

  However, a minimum of 6 increments is always used.

  For multi-carrier tests, each carrier is incremented in 6 equally spaced steps to its fully rated power level. The phase of each carrier is adjusted to maintain the in phase condition. Fast detector diodes and a fast digital storage oscilloscope are used for detection.

Test failure is deemed to have happened if:

- noise spikes recur within 20 % of the power level where they first occurred, after the power was turned off and back on again;
- the noise floor throughout the detection band jumps by more than 10 dB;
- reflected or reverse power suddenly jumps or fluctuates.

A few noise flashes during the initial application of high power are unavoidable in some cases, and does not constitute a failure. These changes are due to a very small amount of foreign material being ionized, or electrical contact changes at waveguide or coaxial interfaces. In the latter case some noise can continue to be generated when the input power or operating temperature are varied. In this situation an alternative method of detection is used to verify if multipaction is occurring or not.

E.2.1.2 Alcatel Espace contribution (phase noise detection method)

This method measures the effect on the phase noise, using a double balanced mixer to remove the amplitude-modulated components from the signal. The noise is measured by a mixer working as a phase detector: this mixer collects on one hand the signal of the TWTA output corresponding to the reference channel (f5), and, on the other hand, the signal filtered at the frequency f5 transmitted by the device under test (via a directive coupler).

The IF DC-signal is detected by an oscilloscope.

This technique has the potential for high sensitivity and is compatible with multi-carrier tests thanks to the use of a large IF bandwidth (DC to 4 GHz) double balanced mixer which allows fast signal detection. This kind of mixer is generally used as a pulse modulated generator and has the ability to provide extremely fast switching times, in the order of one nanosecond.

E.2.2 Return loss

E.2.2.1 Bosch Telecom contribution (nulling selection method)

The forward-reverse power nulling detection method is a well-proven technique which can be used in either CW or pulsed mode for single or multi-carrier multipaction testing.

The nulling is a global detection method, where the incident power to a DUT is nulled against the reflected power. A multipaction discharge creates an imbalance leading to a loss of the null.

The principal arrangement of a multi-carrier nulling circuit is shown in Figure E-2.

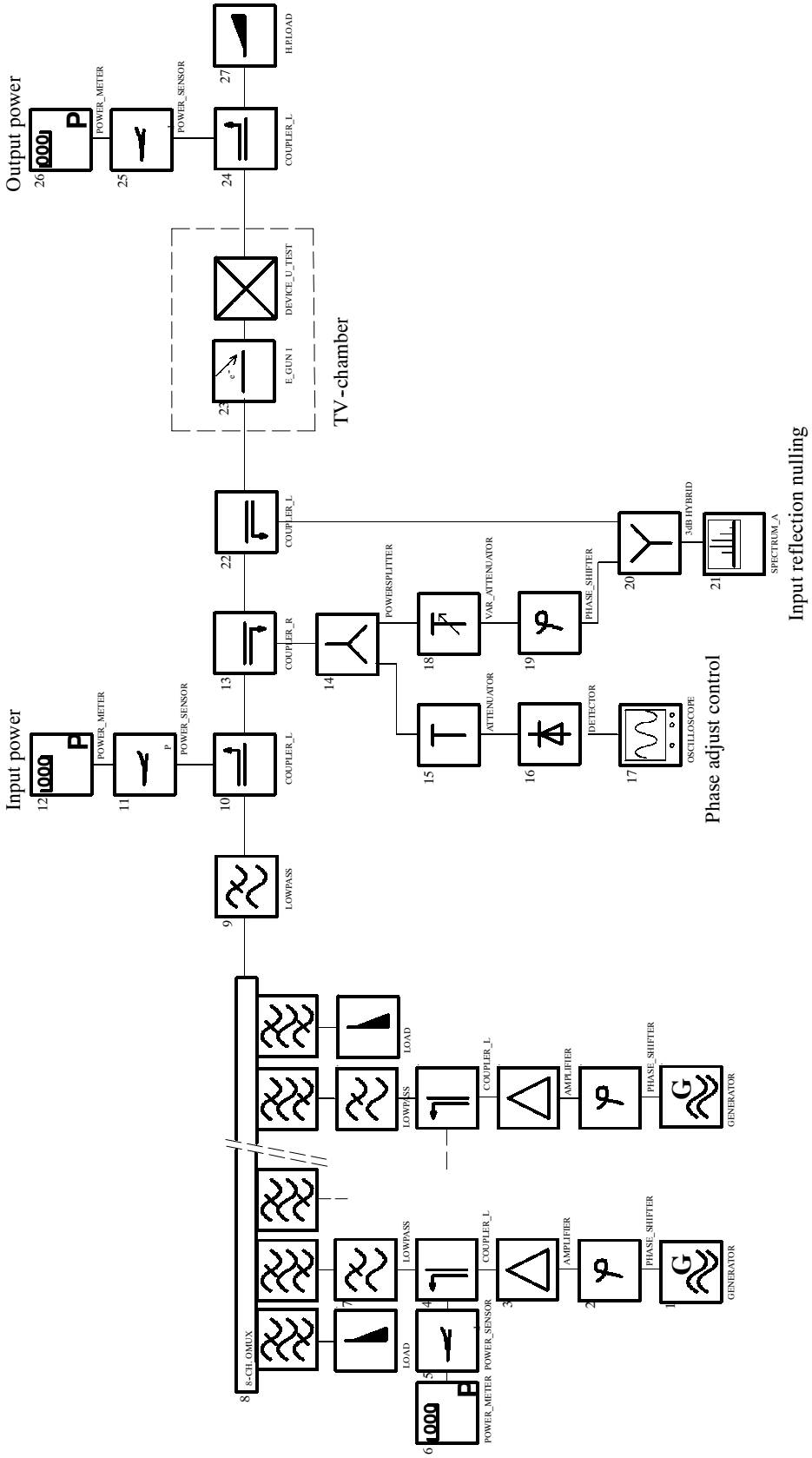

Figure E-2: Principal multipaction test set-up for nulling detection method

A reference signal is coupled from the incident power at coupler R and applied to the nulling hybrid. The reflected power from the DUT is coupled at coupler 22 and also applied to the hybrid. A nulling condition is adjusted with a phase-shifter and a variable attenuator. The null-depth can be monitored on the spectrum analyser.

The spectrum analyser is set to a 200 kHz span and a resolution bandwidth of 10 kHz.

When performing a multi-carrier multipaction test, at first the phase conditions of all carriers are adjusted until the well-known peak-voltage envelope signal is obtained.

In a second step the spectrum analyser is tuned to the centre channel of all applied channels. Then the nulling can be performed, starting with the phase adjustment, until the maximum null-depth is obtained.

The typical null-depth which can be achieved is about -60 dBc.

NOTE 1 This detection method is not suitable for non-reciprocal devices such as isolators.

NOTE 2 A disadvantage of this method is that, due to changes in temperature of the DUT, an optimum null can be achieved only by frequently retuning the system..

NOTE 3 Bosch Telecom experience is that from all detection methods using spectrum analysers (as third harmonic and noise level detection) the nulling method seems to be the most sensitive one.

E.2.2.2 Alcatel Espace contribution (VSWR amplitude and phase variation method)

The multipaction phenomenon creates a variation of the VSWR which is measured by a network analyser.

The reference signal f5 (centre frequency of the OMUX) is connected to the reference port of the analyser and the signal reflected by the device under test is connected to the measurement port of the analyser, via a filter centred on the reference frequency f5.

The techniques described above are similar in that both use a reference and the reflected signal; the difference lies in the method of processing the data. In the first method described, using a nulling technique, phase and amplitude adjustment and signal combination are performed before detection. The second method performs signal comparison at baseband after detection. The former is likely to be more sensitive, and does not rely on a wide measurement dynamic range. However, the latter has the advantage that frequent adjustment of the nulling circuit need not be performed.

E.2.3 Harmonic noise

E.2.3.1 Introduction

The detection of noise at the third harmonic of the carrier frequency has often been used for multipaction testing. The following information on a test method for the detection of this signal was supplied by Alcatel Espace.

E.2.3.2 Third harmonic detection

The multipaction phenomenon generates harmonics of the carriers, which can be detected.

The measurement of the PIMP is done before or after the device under test, thanks to a directive coupler measuring the reflected or transmitted wave followed by a third harmonic transmission filter (WG22 waveguide). The guide after the DUT is a WG 17 one (recommended band 10GHz to15 GHz) so this detection is put as

close as possible to the DUT in order to keep a good sensitivity. The detection is performed by use of a fast rise time diode preceded by a LNA.

The output signal is monitored by a fast digital oscilloscope.

E.3 Transient tests methods

E.3.1 Introduction

This subclause describes the test method used by Astrium in an investigation of multi-carrier multipaction (see reference [18]), and is extracted from the project final report (see reference [4]). The investigation was managed by AEA Technology, who also performed the complementary computational modelling tasks. The work was performed under contract to ESA.

Three variants on the experimental set-up were used:

- For peak powers of less than 4 kW, the test system was configured as shown in Figure E-3 (mode 1).
- For CW operation at power levels in excess of 4 kW the arrangement in Figure E-3 was used in conjunction with a resonant ring power multiplication loop set up in the vacuum chamber.
- When peak powers of greater than 4 kW were used, the system was reconfigured to combine the carriers in an OMUX, this is shown in Figure E-4 (mode 2).

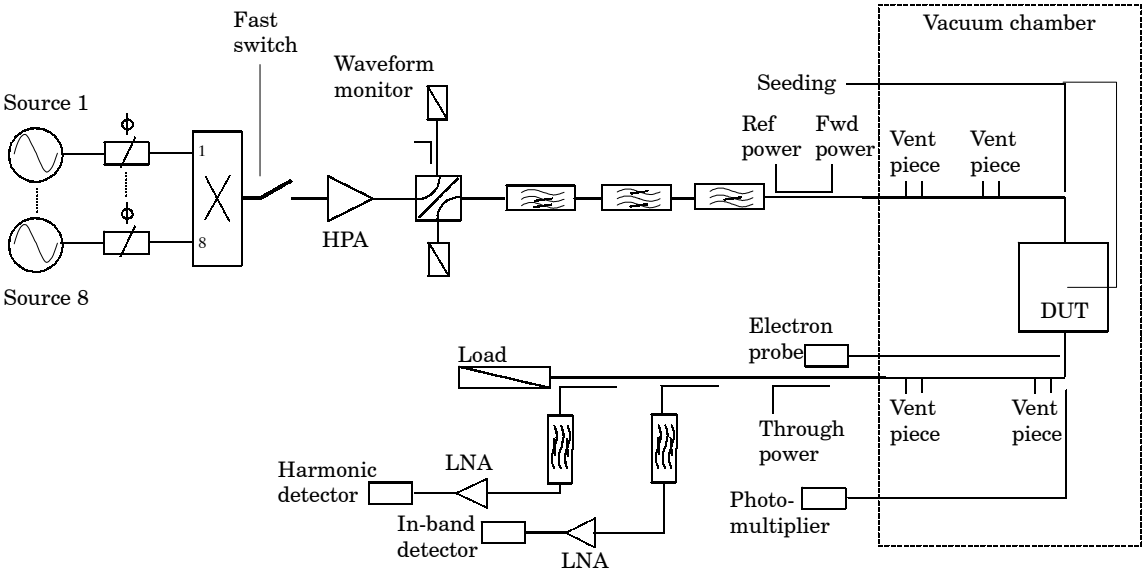

Figure E-3: Test configuration (mode 1)

The combination of test configurations enables a relatively flexible operation. This enables a range of signal waveforms to be applied to the device under test by varying the number of carriers and their frequency spacing.

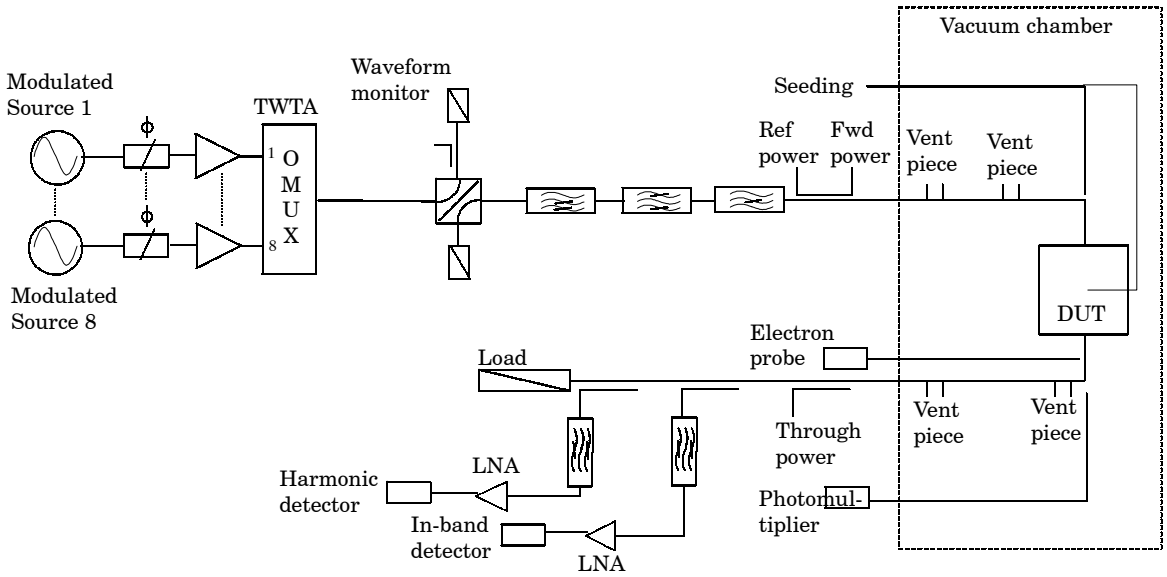

Figure E-4: Test configuration (mode 2)

E.3.2 Signal generation

E.3.2.1 Overview

The individual carriers are generated from separate synthesized sources, which are all phase locked to a common 10 MHz reference signal. Each low power carrier passes through a phase adjuster to ensure that when operating in a multi-carrier test, the carriers can each be phase aligned to obtain the maximum peak power. All multi-carrier frequency plans are centred at 11,1 GHz and the harmonic detector is tuned to the 3rd harmonic of this frequency.

E.3.2.2 Low power combining (mode 1)

In mode 1 operation, low power carriers are combined in an 8–1 way combining network (power divider used in reverse). The combined multi-carrier signal is then modulated, by means of a fast rise time pin diode switch, before being applied to the high power amplifier (HPA). The switch-HPA combination gives a rise time at the output of the HPA of approximately 4 ns. The HPA consists of an array of 8 × 500 W travelling wave tube amplifiers (TWTA) combined together to generate a high power signal across the 8 GHz – 18 GHz band.

The HPA (mode 1) enables the amplification of a single 4 kW CW carrier or a composite multi-carrier waveform up to a peak power of 4 kW. With a multi-carrier signal each individual TWTA handles the whole composite signal waveform and output power is constrained by voltage limiting within individual TWTAs. Because all the carriers pass through an individual TWTA together, they suffer almost identical phase shifts if the electrical length of the TWTA alters due to thermal effects; so the stability of the shape of the composite waveform in the time domain (in particular the amplitude and width of the main peak) is largely a matter of the stability of the synthesizers.

E.3.2.3 High power combining (mode 2)

Test pieces with larger gap peak powers in excess of 4 kW are driven to reach and exceed the multipaction threshold. Although more TWTAs were available, they only enables the peak power to be increased to about 5 kW. The mode 2 system described here peak powers of up to 50 kW to be attained.

In the mode 2 arrangement, each individual carrier is amplified in its own dedicated TWTA. The TWTA outputs are combined at high power in an OMUX. The OMUX used has 11 channels available, of which ten are used. In this way, peak

output powers of $10^2 \times 500$ W or 50 kW are obtained at the expense of some inflexibility in available frequency plans.

In this arrangement each carrier is amplified in a separate TWTA and the composite waveform is assembled in the OMUX. Each carrier suffers the phase shift of its particular TWTA and, if this changes with time, there is no guarantee that all the TWTAs can track. In practice, it is found that the whole array is only stable for a short time under CW conditions. This stability is improved by reducing the mean output power of the TWTAs operating them at a 6,3 % duty cycle (37 μs pulse, 1,7 kHz repetition rate).

The duty cycle is arranged by pulse modulating individual carriers with pin diode modulators driven from a common source. Phase adjustment per carrier is provided prior to the TWTA.

E.3.2.4 Carrier phasing

During multi-carrier testing, a waveguide switch placed at the output of the HPA/OMUX is used to tune the multi-carrier waveform into a load rather than into the test piece. This enables the waveform to be correctly phased and set to the correct amplitude before being applied to the test piece.

E.3.2.5 Filtering

From previous work carried out at ESTEC, it is known that harmonic generation is a side effect of multipaction and can be reliably used as a diagnostic indication. TWTAs generate high levels of third harmonic and the TWTA output was filtered to prevent the third harmonic detector from being desensitized by the TWTA harmonic. Initial investigations indicate that the harmonic levels generated by a multipaction discharge are very low, so a high order of filtering is specified to protect the detector sensitivity.

Other unwanted signals, including higher harmonics and intermodulation products, are removed by means of a bandpass filter. To enable the detection of noise produced close to the carrier, a narrow notch is placed in the system noise floor by a high order bandstop filter, before the test piece.

E.3.2.6 Waveform monitoring

The monitoring of the composite waveform is arranged using a tunnel diode detector loaded to produce a very fast rise time of approximately 1 ns. The output is monitored by a digital storage scope offering a 5 gigasamples/s, 1 GHz bandwidth single shot performance. A typical multi-carrier waveform, as monitored on the oscilloscope, is shown in Figure E-5. The continuous monitoring of the waveform ensures that the phase can be continuously adjusted to maintain the peak power for the duration of the tests.

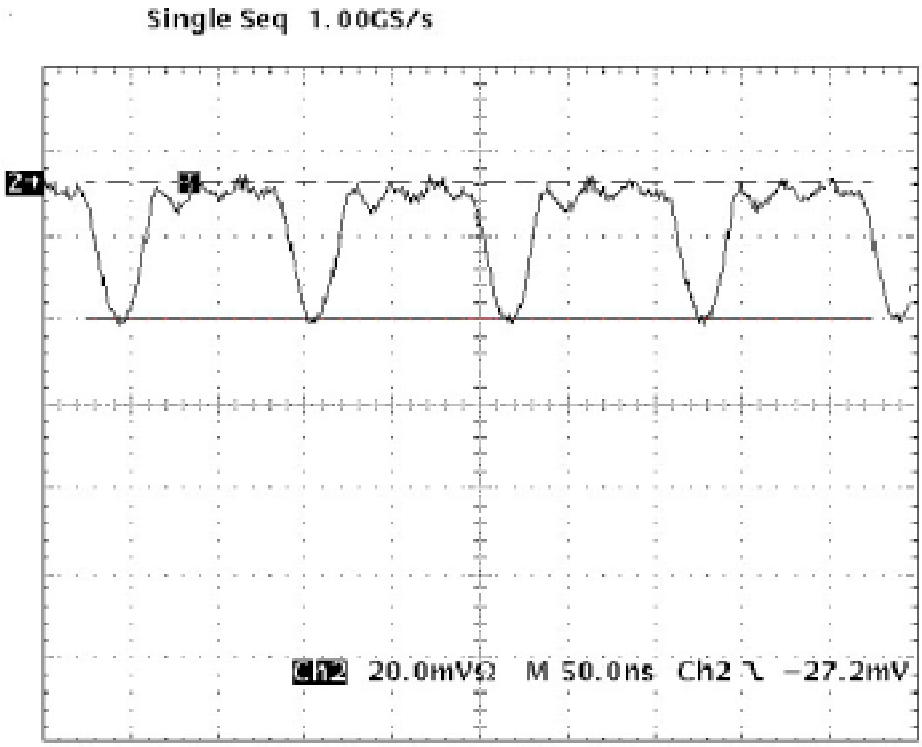

Figure E-5: Detected envelope of a five carrier waveform

E.3.2.7 Multipaction detection methods

Three main detection methods are used in the measurement programme,

- close-to-carrier noise,
- third harmonic output, and
- optical emission.

These are supported by a charge probe and mass spectrometer, which are used for diagnostic purposes as they are too slow for detecting fast transient multipaction events.

E.3.2.8 Spectrum analyser

Initial observations show that a spectrum analyser has a number of limitations as a method of detection for both close-to-carrier noise and harmonic output.

The response time of the analyser is not fast enough to detect short duration events, which can only be a few nanoseconds in duration with multi-carrier signals.

The analyser does not produce an indication of the maximum and average noise associated with the discharge due to the time used to sweep the bandwidth of the filter to give the requested sensitivity.

E.3.2.9 Fast detectors

One of the aims of the measurement programme was to find and make use of detectors with sub-nanosecond rise time. For the detection of the close-to-carrier noise and harmonics, a tunnel diode detector was chosen which had a fast rise time with a reasonable degree of sensitivity, so as not to limit the dynamic range of the detection system. Ideally, operation of the diode into a low output impedance is a condition to produce a fast rise time, but this greatly reduces the sensitivity. The DC signal generated by the diode can be amplified using a video amplifier, but this

greatly increases the overall rise time. The problem is solved by using a low noise amplifier (LNA) at the input to the diode amplifying the signal prior to detection. The condition for the LNA is to have a rise time comparable to that of the diode to maintain the overall detection response time. HEMT LNAs, which have a rise time of a few ps were chosen.

E.3.2.10 Data acquisition

Having produced detectors with very short rise times (approximately1 ns), the next step is to monitor the outputs in real time. This is achieved by using a fast digital storage oscilloscope, operating in single acquisition mode, with a time resolution of 200 ps/division. The oscilloscope is able to capture up to 80 screens of data in a single acquisition, and offers post-measurement scanning through the captured data.

The oscilloscope is triggered, to begin storage, by the third harmonic signal. This enables the observation of changes in the intensity of the discharge with time. The time base is adjusted to try to ensure that a high percentage of the pulse length is captured on the oscilloscope, so that the maximum and average noise levels are representative of the complete pulse width. This is not always easy to do because of long and variable delays between the pulse edge and the onset of a discharge.

E.3.2.11 Close-to-carrier noise

As previously mentioned, a narrow notch is placed in the system noise floor by means of a bandstop filter 200 MHz away from the centre frequency of 11,1 GHz on the input side of the test piece. On the output side of the test piece, a 4 port 20 dB coupler is used to sample the signal and the range of frequencies corresponding to the notch selected by a bandpass filter are amplified by an LNA and detected by a tunnel diode detector. The diode detector has a dynamic range limited to approximately 40 dB, by the trade-off between sensitivity and speed.

E.3.2.12 Harmonic output

The harmonic noise emanating from the HPA is reduced to the specification level by a lowpass filter at the input to the test piece. The harmonic signal from the output of the test piece is coupled from the main RF path by a WG17 coupler, with a known coupling figure at 33,3 GHz, which is the third harmonic frequency. The fundamental and harmonic signals are then separated by a WG17-WG22 tapered transition which offers a high degree of isolation against the fundamental signal. The bandwidth of the WG22 part of the system is defined by a bandpass filter centred on 33,3 GHz, amplified by a HEMT LNA and detected by a tunnel diode detector. The dynamic range of the diode is again restricted to approximately 40 dB, limited by the output impedance used for fast rise time operation.

E.3.2.13 Optical detector

The optical detector consists of a UV transmissive quartz fibre optic mounted in the centre of the sidewall of a waveguide bend. The bend is directly attached to the test piece so that the fibre's field of view is along the length of the test piece, monitoring the reduced height centre section. The light generated by the discharge is predominantly UV; this is detected by means of a photomultiplier tube located outside the chamber operating in the UV region.

The tube and its housing are placed inside a metal box to reduce the light leakage into the tube itself and increase the sensitivity by reducing the dark current.

Although the tube itself has a fairly fast rise time of approximately 4,5 ns, it has a slow initial response time (delay); the difference in response time between the tunnel diode detectors and the optical detector is of the order of hundreds of ns, depending upon the loading of the tube output.

For this reason the harmonic and close-to-carrier noise are used as the principal discharge intensity diagnostics and the optical emissions are used as an auxiliary indication.

E.3.2.14 Charge probe

The rapid increase in the charge density at the onset of multipaction can be used to provide diagnostic information. To monitor the electron density within the wave guide, a small probe biased at 60 V is introduced into the waveguide on the centreline of the narrow wall. A picoameter is then used to monitor the current as an indication of the electron density. This form of detector is inherently slow because of the rise time associated with the amplifier circuit. The detector is mostly used for diagnostic purposes rather than as a detection method because of its slow response time. The detector is shown in Figure E-6.

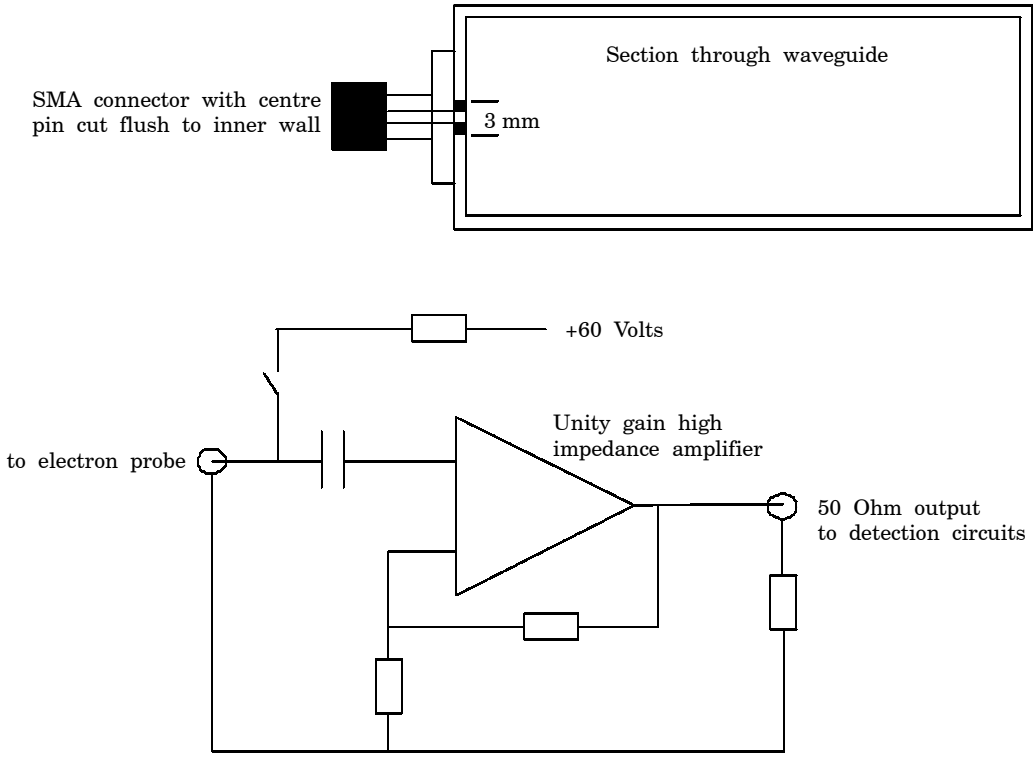

Figure E-6: Charge probe

E.3.2.15 Mass spectrometer

Included within the vacuum chamber is a mass spectrometer which is again used as a diagnostic tool rather than a detector for multipaction due to its slow response time.

E.3.2.16 Free-electron seeding

Prompted by the success at ESTEC in using ultraviolet (UV) light incident on a metal surface as a seeding method, it is proposed to implement this technique on the test set-up. The UV is generated by a calibration lamp at a wavelength of 253,7 nm; this is collimated into a 1,8 mm quartz fibre optic via a collimating lens. The fibre passed through the chamber port plate via a potted feedthrough and introduced the UV into the test piece in one of two ways (see ref [19]):

- The UV can be injected directly into the reduced height section of the test piece through a 1 mm hole drilled in the centre of the broad wall from above.
- The UV can be directed along the horizontal centre line of the test piece in the direction of propagation through a hole drilled in the narrow wall of a

waveguide bend located directly prior to the test piece. The intensity of the lamp was controlled by adjusting the current from the power supply.

E.4 Test facility validation

Separately from any issues of calibration, the test is not complete without a demonstration and validation that the test configuration was functioning correctly immediately prior to and after test. This is because the usual criterion for a successful test is a null result, i.e. that nothing is detected by the detection system.

A way of achieving such a validation is as follows:

- Firstly, validate that the test site with no device under test in place does not generate any signs of multipaction when subjected to full maximum power. This is done in steps of 1 dB from 3 dB below maximum power.
- Secondly, undertake tests with a standard multipaction generator in the vacuum chamber. This item can be a simple component that was designed for multipaction at a power level 3 to 6 dB below the peak power level for the test. Before, after and sometimes during the test sequence, the standard can be switched into the circuit and the correct functioning of the detectors observed at the expected power level.

Bibliography

[1] *A. Woode & J. Petit,* Diagnostic Investigations into the Multipactor Effect, Susceptibility Zone Measurements and Parameters Affecting A Discharge, *ESTEC Working Paper 1556, November 1989.*

[2] *Abstract Book,* Workshop on Multipaction and Passive Intermodulation Products Problems in Spacecraft Antennas, *ESTEC, December 1990.*

[3] *Final Presentations & Working Meeting:* Multipactor & PIM in Space RF Hardware, *ESTEC, January 1993.*

[4] *A. J. Marrison, R. May, J.D. Sanders, A.D. Dyne, A.D. Rawlins, J. Petit,* A study of Multipaction in Multicarrier RF Components, Report no AEA/TYKB/31761/01/RP/05 *Issue 1, January 1997.*

[5] *A.J. Hatch and H.B. Williams,* J. Appl. Phys. ***25****, 417 (1954).*

[6] *A.J. Hatch and H.B. Williams,* Phys. Rev. ***112****, 681 (1958).*

[7] *R. Woo,* Multipacting Discharges between Coaxial Electrodes, *J. Appl. Phys.* ***39****, 1528-1533 (1968).*

[8] *R. Woo,* Final Report on RF Voltage Breakdown in Coaxial Transmission Lines, *JPL Technical Report 32-1500, October 1970.*

[9] *F. Höhn, W. Jacob, R. Beckmann, R. Wilhelm,* The Transition of a Multipactor to a low-pressure gas discharge, *Phys. Plasma,* ***4****, 940-944 (1997).*

[10] *J.M. Meek and J.D. Craggs,* Electrical Breakdown of Gases, *Wiley (1978).*

[11] *L. Galan et al.,* Study of Secondary Electron Emission Properties of Materials for High RF Power in Space, *UAM Final Report, ESTEC Contract 6577/85, July 1990.*

[12] *W. Arter and M.P. Hook,* Multipaction Threshold Curves for Coaxial Geometries, *AEA Technology Report AEA/TYKB/28046/RP/1, 1997.*

[13] *L. Galan et al.,* Study of secondary emission properties of materials used for high power rf components in space, *Technical Report, ESTEC 1987.*

[14] Méthode de synthèse de réseaux linéaires et plans rayonnant un diagramme a contour formé, *Thesis presented by Cyril MANGENOT on November 30, 1989.*

[15] *C. Phillips, A. Woode, P. Woodhouse,* A multpactor investigation program at C-band, *Estec Working Paper No. 1412, ESA 1985*

[16] *J. Petit,* Measurements performed on the ERS-1 structural model switching matri, *ESTEC Internal Memo TRI/042/JP*

[17] The detection of organic contamination of surfaces by infra-red spectroscopy. *ESA PSS-01-705 Issue 1.*

[18] A Study of Multipaction in Multicarrier RF Components, *ESA/ESTEC contract number 10873/94/NL/DS.*

[19] *D. Raboso and A. Woode, EUMC'95* "A new method of electron seeding used for accurate testing of multipactor transients".

ECSS Document Improvement Proposal

1. Document I.D.	2. Document date	3. Document title
ECSS-E-20-01A	5 May 2003	Multipaction design and test

4. Recommended improvement (identify clauses, subclauses and include modified text or graphic, attach pages as necessary)

5. Reason for recommendation

6. Originator of recommendation

Name:	Organization:	
Address:	Phone: Fax: e-mail:	**7. Date of submission:**

8. Send to ECSS Secretariat

Name:	Address:	Phone: +31-71-565-3952
W. Kriedte ESA-TOS/QR	ESTEC, P.O. Box 299 2200 AG Noordwijk The Netherlands	Fax: +31-71-565-6839 e-mail: Werner.Kriedte@esa.int

Note: The originator of the submission should complete items 4, 5, 6 and 7.

An electronic version of this form is available in the ECSS website at: http://www.ecss.nl/
At the website, select “Standards” - “ECSS forms” - “ECSS Document Improvement Proposal”

(This page is intentionally left blank)